A Unified Approach to Synchronization Problems over Subgroups of the Orthogonal Group

Huikang Liu[*] Man-Chung Yue[†] Anthony Man-Cho So[‡]

September 17, 2020

Abstract

Given a group $\mathcal{G}$, the problem of synchronization over the group $\mathcal{G}$ is a constrained estimation problem where a collection of group elements $G_1^*, \ldots, G_n^* \in \mathcal{G}$ are estimated based on noisy observations of pairwise ratios $G_i^* {G_j^*}^{-1}$ for an incomplete set of index pairs (i, j). This problem has gained much attention recently and finds lots of applications due to its appearance in a wide range of scientific and engineering areas. In this paper, we consider the class of synchronization problems over a closed subgroup of the orthogonal group, which covers many instances of group synchronization problems that arise in practice. Our contributions are threefold. First, we propose a unified approach to solve this class of group synchronization problems, which consists of a suitable initialization and an iterative refinement procedure via the generalized power method. Second, we derive a master theorem on the performance guarantee of the proposed approach. Under certain conditions on the subgroup, the measurement model, the noise model and the initialization, the estimation error of the iterates of our approach decreases geometrically. As our third contribution, we study concrete examples of the subgroup (including the orthogonal group, the special orthogonal group, the permutation group and the cyclic group), the measurement model, the noise model and the initialization. The validity of the related conditions in the master theorem are proved for these specific examples. Numerical experiments are also presented. Experiment results show that our approach outperforms existing approaches in terms of computational speed, scalability and estimation error.

Keywords: Group Synchronization, (Special) Orthogonal Matrix, Permutation Matrix, Cyclic Group, Generalized Power Method, Estimation Error

[*]Imperial College London. E–mail: `huikang.liu@imperial.ac.uk`
[†]The Hong Kong Polytechnic University. E–mail: `manchung.yue@polyu.edu.hk`
[‡]The Chinese University of Hong Kong. E–mail: `manchoso@se.cuhk.edu.hk`

1 Introduction

In many real-world estimation problems, the signals of interest are constrained to lie in a *group*[1]. One such example is the *group synchronization problems* (or simply called *synchronization problems*) where a collection of group elements are estimated based on noisy pairwise ratios of the elements. More precisely, the synchronization problem over a group $\mathcal{G}$ consists of estimating n group elements $G_1^*, \ldots, G_n^* \in \mathcal{G}$, together called the *ground truth*, based on noisy observations of pairwise ratios $G_i^* G_j^{*-1}$ (with respect to the binary operation of the group $\mathcal{G}$) for some index pairs $(i, j) \in [n]^2$.

Synchronization problems have found applications across a wide range of areas, such as social science, distributed network, signal processing, computer vision, robotics, structural biology, computational genomics and machine learning, and hence gained much attention over the past decade. Indeed, many important problems from the above areas can be formulated as a group synchronization problem, including community detection [3, 15] where $\mathcal{G}$ is the Boolean group; ranking [16] and distributed clock synchronization [19] where $\mathcal{G}$ is the group of 2D rotations; sensor network localization and cryo-electron microscopy where $\mathcal{G}$ is the group of orthogonal matrices or special orthogonal matrices [17, 39]; the pose graph estimation problem [37] where $\mathcal{G}$ is the group of Euclidean motions; the haplotype phasing problem [13, 40] where $\mathcal{G}$ is the cyclic group (integers with modulo arithmetics); and the multi-graph matching problem [22, 33] where $\mathcal{G}$ is the group of permutations.

Numerical approaches to synchronization problems are roughly divided into three categories: the spectral estimator, the SDP relaxation and the non-convex approach. In the context of synchronization problems, the spectral estimator was first introduced in [41] for phase synchronization (*i.e.*, $\mathcal{G}$ is the group $\mathcal{SO}(2)$ of 2D rotations). It has later been generalized to synchronization problems over other subgroups of the orthogonal group, see [1, 6, 27, 33], and even over general compact groups [35]. The main computational cost of this approach comes from two parts. First, the eigenvectors corresponding to the first few eigenvalues of the *graph connection Laplacian* [6] or a data matrix C constructed using the noisy observations (see Sections 2 and 8 for its construction) are computed. Second, a certain rounding procedure is invoked for to ensure that the returned estimator lies in the feasible set $\mathcal{G}^n$. The major advantages of the spectral estimator are its low computational cost and ease of implementation.

The SDP relaxation approach is based on convex relaxations of either the least squares formulation or the least unsquared deviation formulation of the synchronization problem, which are both non-convex optimization problems. These convex relaxations are semidefinite programming problems (and hence its name) that are obtained via the by-now classic *lifting* technique (see, *e.g.*, [31]) and shown to be tight — the optimal solutions to the

[1] In mathematics, a group is a set together with a binary operation on the set satisfying certain axioms. For example, the set of orthogonal matrices together with the usual matrix multiplication as the binary operation forms a group, called the *orthogonal group*. For the precise definition of a group, readers are invited to [36].

relaxed problem are also optimal for its non-relaxed counterpart — under certain assumptions on the observation and noise models [1, 3, 4, 23, 37, 46]. A major drawback of the SDP relaxation approach is that it does not scale well with n since it requires solving a semidefinite programming problem with an $N \times N$ matrix decision variable, where N is linear in n. Hence, this approach is impractical when a large number of group elements are to be estimated. One remedy to this is to devise specialized optimization algorithms for solving the large SDP problem. For example, an alternating direction augmented Lagrangian method has been developed in [46] solving for a semidefinite programming relaxation of the least unsquared deviation formulation of synchronization problems over the special orthogonal group. However, the computational time is still not satisfactory when the number n of target group elements is beyond a few hundreds. Furthermore, these specialized optimization algorithms often require sophisticated tuning of multiple algorithmic parameters such as the step sizes or the penalty parameter in the augmented Lagrangian term. Another possible remedy is to solve the large SDP problem by using the Burer-Monteiro approach [10, 11], which amounts to replacing the large semidefinite matrix variable $Z \in \mathbb{R}^{N\times N}$ by some factorization $YY^\top$ with $Y \in \mathbb{R}^{N\times f}$ and solving the resulting optimization problem in the smaller matrix variable Y. However, the Burer-Monteiro approach is prone to sub-optimality due to local minima, unless the factorization dimension f is sufficiently large [5, 8, 9, 28].

The non-convex approach directly solves the non-convex least squares formulation without relaxing it. It is a two-stage approach that consists of a carefully designed initialization, which ensures the initial point is close enough to the ground truth, and an iterative refinement procedure via the *generalized power method* (GPM) [24, 30, 32]. The idea of applying GPM to synchronization problems was first introduced in [7] for phase synchronization and then in [13] for the joint alignment problem. Improved analysis of GPM for phase synchronization can be found in [29, 49]. The advantage of the non-convex approach is that it is much faster and more scalable than the SDP relaxation approach since each iteration involves only matrix-vector multiplications and projections onto the group $\mathcal{G}$. As we shall see later, these projections can be computed extremely efficiently for many concrete groups $\mathcal{G}$ of practical relevance. Also, the non-convex approach is easy to implement and requires no parameter tuning. Despite that the spectral estimator has been shown to be already rate-optimal in certain settings [7, 27], as observed in our experiments, the quality of the estimator returned by the non-convex approach initialized by the spectral estimator can be substantially better (see Section 9). In other words, we can greatly improve the performance of the spectral estimator by paying a small amount of extra computational cost.

Interestingly, the spectral estimator approach is an approximation algorithm for the non-convex least squares formulation, in the same spirit as Trevisan's algorithm for the MAX-CUT problem [42]. In fact, syncrhonization over the Boolean group is equivalent to the MAX-CUT problem [46]. The *approximation accuracy* of the spectral estimator (*i.e.*, the gap between the objective value of the spectral estimator and the optimal value) is intimately related to the smallest non-zero eigenvalue of the graph connection Laplacian [6]. However, since the optimal solution to the least squares formulation is in general different from the ground truth, a more relevant and faithful measure for the quality of an estimator to a synchronization problem would be the *estimation error* which is defined as the deviation of the estimator from the ground truth. Results on the estimation errors of the optimal solutions to the least squares formulation and the least unsquared deviation formulation can be found in [4] and [46], respectively. In the case of $\mathcal{SO}(2)$-sync, it has been shown in [29] that GPM produces iterates with decreasing estimation error.

Finally, we remark that a powerful framework has recently been developed in [26] for "cleaning" the input data to general synchronization problems by leveraging the so-called *cycle-edge consistency*. More precisely, let $E \subseteq [n]^2$ be the subset containing all the index pairs (i,j) for which the noisy observation C_{ij} of the ratio $G_i^* G_j^{*-1}$ is available. The pair $([n], E)$ is called the *measurement graph* of the synchronization problem. Unreliable observations C_{ij} are then removed by detecting a certain inconsistency of the observations C_{ij} along cycles on the measurement graph, see [26] for details. It would be interesting to investigate the practical performance of combining our non-convex approach with their framework. We leave this as our future work.

1.1 Contributions

This paper considers synchronization problems over *closed subgroups of the orthogonal group* $\mathcal{O}(d)$, which include, *e.g.*, the orthogonal group $\mathcal{O}(d)$ itself, the special orthogonal group $\mathcal{SO}(d)$, the permutation group $\mathcal{P}(d)$ and the cyclic group $\mathcal{Z}_m$ (see Section 2.1.1 for their definitions). Our contributions are threefold.

- First, we propose a unified, non-convex approach for solving this class of synchronization problems, namely, the GPM with a particular spectral estimator as initialization. Not only is our approach easy to implement but also enjoys faster computational speed and better scalability. Therefore, it is particularly suitable for applications of synchronization problems where the number n of target group elements is large.

- Second, we derive a master theorem for the proposed non-convex approach. Under certain conditions that are related to the group, the noise, the measurement graph and the initialization, the master theorem upper bounds the estimation error of the iterates of the GPM and hence provides performance guarantees for the proposed non-convex approach (see Theorem 1). The master theorem is applicable to general closed subgroups of the orthogonal group, measurement graphs and noise.

- Third, in Sections 5 to 8, we verify the conditions required by the master theorem for concrete subgroups ($\mathcal{O}(d)$, $\mathcal{SO}(d)$, $\mathcal{P}(d)$ and $\mathcal{Z}_m$), a random measurement graph model (the Erdös-Rényi graphs), a noise model (the sub-Gaussian noise) and a particular initialization by a novel spectral estimator. As a consequence of the validity of these conditions, the master theorem provides a strong theoretical guarantee for the performance of our non-convex approach to a large class of practically relevant group synchronization problems. For cyclic synchronization $\mathcal{Z}_m$-sync, another non-convex approach is developed in [13]. However, unlike the one in [13], the dimension of the iterate and computational cost of our non-convex approach do not increase with m. Therefore, ours is much more efficient.

Although the idea of solving synchronization problems using GPM is natural in view of the above discussion, due to the non-commutativity of the orthogonal group $\mathcal{O}(d)$, many of the key steps in [29] that rely on the commutativity of $\mathcal{SO}(2)$ break down. Hence, extending the theoretical results in [29] to synchronization problems over general subgroups of $\mathcal{O}(d)$ is highly non-trivial. Furthermore, the measurement and noise settings in this paper are also significantly more general than those considered in [29].

1.2 Organization

The rest of the paper is organized as follows. We formally introduce the group synchronization problem and some definitions related to it in Section 2. In Section 3, we propose a unified non-convex approach for the class of synchronization problems over closed subgroups of the orthogonal group. We then prove a master theorem on the performance guarantee for the proposed approach in Section 4. There are four conditions required by the master theorem, which are related to the group, the measurement graph model, the noise model and the initialization. Sections 5 and 8 are respectively devoted to the verification of these four conditions by focusing on concrete examples. Section 9 presents numerical experiments on the proposed approach. Finally, we conclude the paper in Section 10.

1.3 Notations

We use the following notations throughout the paper. For any $nd \times nd$ ($nd \times d$) block matrix Y, we denote by $[Y]_{ij}$ ($[Y]_i$) its ij-th (i-th) $d \times d$ block. For two matrices X and Y of conformable dimensions, $\langle X, Y\rangle = \mathrm{Tr}(X^\top Y)$. Also, $\|X\|$ and $\|X\|_F$ denote the operator norm and Frobenius norm, respectively. For any integer $k \geq 1$, the $k \times k$ identity matrix is denoted by I_k. Unimportant numerical constants appeared in mathematical statements and their proofs are denoted by c and c_i, $i \geq 1$. Their values may change from appearance to appearance. For a graph with nodes $[n] := \{1, \ldots, n\}$, we denote by (i, j) its edge between the nodes i and j.

2 Group Synchronization Problems

Let $\mathcal{G} \subseteq \mathbb{R}^{d\times d}$ be a group with matrix multiplication as the binary operation. The problem of *group synchronization over* $\mathcal{G}$, denoted by $\mathcal{G}$-sync, is to estimate some unknown group elements $G_1^*, \ldots, G_n^* \in \mathcal{G}$ of interest based on noisy observations of their pairwise ratios:

$$C_{ij} \approx G_i^* G_j^{*-1}, \quad (i,j) \in E,$$

where $E \subseteq \{(i,j) \in [n]^2 : i < j\}$ is a collection of index pairs. This is a constrained estimation problem and the feasible set is the Cartesian product $\mathcal{G}^n$. We treat the set $\mathcal{G}^n$ as a subset of $\mathbb{R}^{nd \times d}$. The target elements can then be represented collectively as a block matrix $G^* \in \mathcal{G}^n \subseteq \mathbb{R}^{nd \times d}$ with $[G^*]_i = G_i^*$. Note that if we multiply the target elements $G_1^*, \ldots, G_n^*$ by a common group element $Q \in \mathcal{G}$ from the right, the resulting elements $G_1^* Q, \ldots, G_n^* Q$ would yield precisely the same set of measurements since

$$G_i^* Q (G_j^* Q)^{-1} = G_i^* Q Q^{-1} G_j^{*-1} = G_i^* G_j^{*-1}. \tag{1}$$

Therefore, we can at best recover the target elements up to some unknown common transformation $Q \in \mathcal{G}$ from the right. Thus, the *estimation error* $\epsilon(G)$ of any estimator $G \in \mathcal{G}^n$ is defined as

$$\epsilon(G) = \min_{Q \in \mathcal{G}} \|G - G^* Q\|_F. \tag{2}$$

The pair $([n], E)$ forms a graph, called the *measurement graph* of the synchronization problem $\mathcal{G}$-sync. We assume that the measurement graph is connected. To formally model the noisy observations of the pairwise ratios, we suppose that there exist matrices Θ_{ij} for $(i,j) \in E$ such that

$$C_{ij} = G_i^* G_j^{*-1} + \Theta_{ij}. \tag{3}$$

The matrices Θ_{ij} for $(i,j) \in E$ are called the noise matrices of the synchronization problem. The noise model (3) is called the *additive noise model* and adopted frequently in the literature of group synchronization problem, see, *e.g.*, [4, 7, 23, 29, 33, 34, 41]. Another popular noise model is the *multiplicative noise model* [13, 35, 46]:

$$C_{ij} = G_i^* G_j^{*-1} \Theta_{ij}.$$

For compact group $\mathcal{G}$, a special case of the multiplicative noise model is the so-called *outlier noise model* where Θ_{ij} is a random element distributed uniformly over G (*i.e.*, with respect to the *Haar measure*) with a certain probability and otherwise the identity element of $\mathcal{G}$ (*i.e.*, $C_{ij} = G_i^* G_j^{*-1}$). Although the theory in this paper does not cover the case of multiplicative noise model, experiment results indicate that our proposed approach performs very well for both additive and multiplicative noise models.

2.1 Synchronization over Subgroups of $\mathcal{O}(d)$

In this paper, we focus on synchronization problems over closed subgroups of the orthogonal group $\mathcal{O}(d)$ which is defined as

$$\mathcal{O}(d) := \left\{ Q \in \mathbb{R}^{d \times d} : QQ^\top = Q^\top Q = I_d \right\}.$$

This class of synchronization problems covers a wide range of applications, see Section 1.

2.1.1 Some Examples of Closed Subgroups of $\mathcal{O}(d)$

An obvious example of closed subgroups of $\mathcal{O}(d)$ is of course the group $\mathcal{O}(d)$ itself. Another example is the Boolean group $\{+1, -1\}$, in which case $d = 1$. The special orthogonal group $\mathcal{SO}(d)$ is also a closed subgroup of $\mathcal{O}(d)$, which is defined as

$$\mathcal{SO}(d) := \left\{ Q \in \mathbb{R}^{d\times d} : QQ^\top = Q^\top Q = I_d, \det(Q) = 1 \right\}.$$

The fourth example is the permutation group $\mathcal{P}(d)$ which is defined as

$$\mathcal{P}(d) := \left\{ Q \in \{0,1\}^{d\times d} : QQ^\top = Q^\top Q = I_d \right\}.$$

The final example that we present is the cyclic group $\mathcal{Z}_m$ of order m, which is defined as

$$\mathcal{Z}_m := \left\{ \begin{pmatrix} \cos\frac{2k\pi}{m} & -\sin\frac{2k\pi}{m} \\ \sin\frac{2k\pi}{m} & \cos\frac{2k\pi}{m} \end{pmatrix} : k = 0, \ldots, m-1 \right\}.$$

2.1.2 The Least Squares Estimator

For any subgroup $\mathcal{G}$ of the orthogonal group, since $Q^{-1} = Q^\top$ for any $Q \in \mathcal{G}$, the least squares estimation problem associated with $\mathcal{G}$-sync is given as

$$\begin{aligned} \min_{G\in\mathbb{R}^{nd\times d}} \quad & \sum_{(i,j)\in E} \|[G]_i[G]_j^\top - C_{ij}\|_F^2 \\ \text{subject to} \quad & [G]_i \in \mathcal{G}, \ i = 1, \ldots, n. \end{aligned}$$

Any optimal solution[2] to this optimization problem is said to be a least squares estimator to the problem $\mathcal{G}$-sync. By the orthogonality of the blocks $[G]_i$, one can equivalently re-write the least squares estimation problem as

$$\begin{aligned} \max_{G\in\mathbb{R}^{nd\times d}} \quad & \operatorname{Tr}\left(G^\top C G\right) \\ \text{subject to} \quad & G \in \mathcal{G}^n, \end{aligned} \tag{4}$$

where $C \in \mathbb{R}^{nd\times nd}$ is the block matrix defined by

$$[C]_{ij} = \begin{cases} C_{ij} & \text{if } (i,j) \in E, \\ C_{ji}^\top & \text{if } (j,i) \in E, \\ I_d & \text{if } i = j, \\ \mathbf{0} & \text{otherwise.} \end{cases}$$

[2]By the same argument as in (1), it can be seen that the least squares estimator is not unique.

Since problem (4) is non-convex, it is in general hopeless to compute a global minimizer in a reasonable amount of time. Indeed, even in the simplest case that $d = 1$ and $\mathcal{G} = \{+1, -1\}$ is the Boolean group, problem (4) is equivalent to a non-convex quadratically constrained quadratic programming which is known to be NP-hard. A standard idea to tackle problem (4) is to consider its semidefinite programming relaxations [1, 4, 23, 37, 46], which are (convex) semidefinite optimization problems and can be solved by off-the-shelf solvers in polynomial time. However, this approach is impractical as it requires solving a semidefinite programming problem with an $nd \times nd$ matrix variable.

3 The Non-Convex Approach

Instead of convexification, we directly tackle the non-convex problem (4) by a two-stage approach. An important step in our approach is the projection of a $d \times d$ matrix onto the group $\mathcal{G}$. This projection, denoted by Π, is defined as

$$\Pi_{\mathcal{G}}\left(X\right) := \operatorname*{argmin}_{Q \in \mathcal{G}} \|X - Q\|_F = \operatorname*{argmax}_{Q \in \mathcal{G}} \langle\, X, Q\, \rangle, \quad X \in \mathbb{R}^{d \times d}. \tag{5}$$

In other words,

$$\operatorname{dist}(X, \mathcal{G}) := \min_{Q \in \mathcal{G}} \|X - Q\|_F = \|X - \Pi_G(X)\|_F.$$

Using the projection $\Pi_{\mathcal{G}}$, we can send any $nd \times d$ matrix onto the feasible region $\mathcal{G}^n$ of the synchronization problem via the *block-wise projection* $\Pi_{\mathcal{G}}^n$. Specifically, $\Pi^n : \mathbb{R}^{nd \times d} \to \mathcal{G}^n$ is the mapping[3] defined as

$$\left[\Pi_{\mathcal{G}}^n\left(Y\right)\right]_i = \Pi_{\mathcal{G}}\left([Y]_i\right) \quad \forall i = 1, \ldots, n.$$

From now on, we omit the subscript $\mathcal{G}$ from the notations $\Pi_{\mathcal{G}}^n$ and $\Pi_{\mathcal{G}}$ if the group $\mathcal{G}$ is clear from the context. We record a useful property of the projection Π before we move on.

Lemma 1. *For any matrix $X \in \mathbb{R}^{d \times d}$ and any scalar $\eta > 0$, it holds that*

$$\Pi(\eta \cdot X) = \Pi(X).$$

The proof of Lemma 1 is straightforward and thus omitted.

We can now describe the details of the two stages of our approach. The first stage aims at finding a feasible point $G^0 \in \mathcal{G}^n$ that has a sufficiently small estimation error $\epsilon(G^0)$. Theorem 1 below provides an explicit upper bound on the estimation error $\epsilon(G^0)$ that our non-convex approach requires. In Section 8, we propose a novel spectral estimator for

[3]Strictly speaking, $\Pi_{\mathcal{G}}^n$ and $\Pi_{\mathcal{G}}$ are not mapping as in general there can be multiple minimizers to the minimization problem in the definition. However, when there are multiple minimizers, all the results in this paper hold by taking an arbitrary one.

general group synchronization problems and show that under certain stochastic models for the measurements and noise, the proposed spectral estimator satisfies the said upper bound on the estimation error with overwhelming probability and hence can be used as G^0 in the first stage. Furthermore, the proposed spectral estimator can be computed efficiently.

In the second stage, starting with the initial point G^0 obtained from the first stage, we iteratively refine the estimates by using the following generalized power method.

Algorithm 1 Generalized Power Method for $\mathcal{G}$-sync

1: **Input:** The matrix C and the initial point G^0.
2: **for** $t = 0, 1, 2, \ldots$ **do**
3: $\quad G^{t+1} = \Pi^n(CG^t)$.
4: **end for**

The name generalized power method of Algorithm 1 comes from its close resemblance with the classical power method [20] for computing the dominant eigenvector of a matrix. In fact, problem (4) can be seen as a constrained eigenvalue problem. More precisely, in problem (4), each column v of G is not only normalized to a fixed length ($\|v\|_2 = \sqrt{n}$ in this case) and orthogonal to all other columns, as in the usual eigenvalue problem, but also subject to an extra constraint that the d-dimensional sub-vectors $v_{1:d}, v_{d+1:2d}, \ldots, v_{(n-1)d+1:nd}$ are all of unit length (here the MATLAB notation $v_{k:\ell}$ for denoting the sub-vector $(v_k, \cdots, v_\ell)^\top$ of v is used). Despite this resemblance, solving group synchronization problems and analyzing the generalized power method are highly non-trivial, owing to the extra non-convex constraints.

Overall, the proposed non-convex approach enjoys several computational advantages and is very efficient. The main cost for computing the spectral estimator lies in the computation of the first d eigenvectors of the matrix C, which can be done efficiently by a host of modern eigen-solvers. As for the second stage, we can see from Algorithm 1 that the GPM has no tuning parameters and can be implemented extremely easily. The computational cost at each iteration consists of two parts: d matrix-vector multiplications for forming the product CG^t and the block-wise projection Π^n which can be decomposed into n projections Π onto the group $\mathcal{G}$. Therefore, the GPM is well-suited for parallelization. As we will see in Section 5, for the orthogonal group $\mathcal{O}(d)$, the special orthogonal group $\mathcal{SO}(d)$ and the permutation group $\mathcal{P}(d)$, the projection Π reduces to a d-dimensional linear programming problem or singular value decomposition. Also, for the cyclic group $\mathcal{Z}_m$, the projection Π can also be computed using a simple, explicit formula involving trigonometric functions. Numerical experiments in Section 9 also demonstrates the superior computational speed and scalability of the proposed approach.

4 A Master Theorem

We present a master theorem on the estimation performance of the non-convex approach. Towards that end, we need the following notations. Let $\bar{E} = E \cup \{(1,1), \ldots, (n,n)\}$. Then, every node of the graph $([n], \bar{E})$, called the *extended measurement graph*, has precisely one self-loop. Let $w_{ij} = 1$ if either $(i,j) \in \bar{E}$ or $(j,i) \in \bar{E}$; otherwise $w_{ij} = 0$. The degree r_i of node i of the extended measurement graph is then given by $r_i = \sum_{j=1}^n w_{ij}$. Note that for any $i \in [n]$, $r_i \geq 1$ since $w_{ii} = 1$. For $j,k = 1, \ldots, n$, let $\mu_{jk} = \sum_{i=1}^n \frac{w_{ij} w_{ik}}{r_i^2}$. We define the following parameters for the measurement graph:

$$\kappa_1 = n \cdot \max_{j<k} \left| \mu_{jk} - \frac{1}{n} \right|, \quad \text{and} \quad \kappa_2 = \max_{j=1,\ldots,n.} \left(\mu_{jj} - \frac{1}{n} \right) \quad \text{and} \quad \kappa = \kappa_1 + \kappa_2.$$

The parameters κ_1 and κ_2 (and hence κ) are related to the connectedness of the measurement graph $([n], E)$, see the discussion after Theorem 1. We also let $D \in \mathbb{R}^{nd \times nd}$ be the diagonal matrix given by $D = \operatorname{BlkDiag}(r_1 \cdot I_d, \ldots, r_n \cdot I_d)$ and $\Delta \in \mathbb{R}^{nd \times nd}$ the block matrix defined by, for $i,j = 1, \ldots, n$,

$$[\Delta]_{ij} = [C]_{ij} - w_{ij} \cdot \left[G^* G^{*\top} \right]_{ij} = \begin{cases} C_{ij} - G_i^* G_j^{*\top} & \text{if } (i,j) \in E, \\ C_{ji}^\top - G_i^* G_j^{*\top} & \text{if } (j,i) \in E, \\ \mathbf{0} & \text{otherwise.} \end{cases}$$

For any $t \geq 0$, we define

$$Q^t := \operatorname*{argmin}_{Q \in \mathcal{G}} \left\| G^t - G^* Q \right\|_F = \operatorname*{argmax}_{Q \in \mathcal{G}} \langle G^{*\top} G^t, Q \rangle = \Pi \left(G^{*\top} G^t \right), \tag{6}$$

where the last equality follows from the definition (5) of Π. Thus, $\epsilon(Q^t) = \left\| G^t - G^* Q^t \right\|_F$ for all $t \geq 0$.

The following theorem is the first main theoretical result of this paper, which shows that under certain conditions, the estimation error of the iterates of the proposed non-convex approach enjoys an increasingly better bound.

Theorem 1 (Master Theorem for GPM)**.** *Suppose that the following hold:*

(i) there exists $\rho \geq 1$ such that for any $t \geq 0$,

$$\|G^{*\top} G^t - n \cdot Q^t\|_F \leq \rho \cdot \operatorname{Tr}(n \cdot I_d - Q^{t\top} G^{*\top} G^t);$$

(ii) $\kappa \leq \frac{1}{1024}$;

(iii) $\left\| D^{-1} \Delta \right\| \leq \frac{1}{32}$ and $\left\| D^{-1} \Delta G^* \right\|_F \leq \frac{\sqrt{n}}{32\rho}$;

(iv) $\epsilon(G^0) \le \frac{\sqrt{n}}{2\rho}$.

Then, it holds that

$$\epsilon(G^t) \le \left(\frac{5}{8}\right)^{t+1} \epsilon(G^0) + \frac{16}{3} \left\| D^{-1} \Delta G^* \right\|_F \quad \forall t \ge 1.$$

We discuss the assumptions and implication of Theorem 1 before we prove it. Condition (i) reflects the geometry of the subgroup $\mathcal{G}$ through the projection map Π_G. When $\mathcal{G}$ is the orthogonal group $\mathcal{O}(d)$, the special orthogonal group $\mathcal{SO}(d)$, or the permutation group $\mathcal{P}(d)$, we can take $\rho = 1$, see Section 5. We conjecture that condition (i) is actually true for arbitrary closed subgroups of the orthogonal group, see Conjecture 1. Condition (ii) is related to the measurement graph $([n], E)$ and represents the requirement that the measurement graph needs to be sufficiently connected. In particular, $\kappa = 0$ when the measurement graph is a complete graph (*i.e.*, $w_{ij} = 1$ for all $i < j$). Condition (iii) depends on both the measurement graph (through the matrix D) and the noise model (through the matrix Δ). Roughly speaking, modulo the effect of D, this condition requires that the measurement noise cannot be too large. For the special case of $\mathcal{SO}(2)$-sync with a complete measurement graph, a similar condition is used in the analysis of the SDP relaxation approach, see [4, Definition 3.1]. Condition (iv) captures the requirement that the GPM needs to be initialized with a point G^0 of sufficiently small estimation error.

The result of Theorem 1 (with condition (iii)) implies that, as $t \to \infty$,

$$\epsilon(G^t) \le \frac{16}{3} \left\| D^{-1} \Delta G^* \right\|_F \le \frac{\sqrt{n}}{6\rho}. \tag{7}$$

It may seem that the bound (7) does not improve by much the bound $\frac{\sqrt{n}}{2\rho}$ on the initial estimation error. However, the numerical constants $\frac{1}{32}$, $\frac{5}{8}$ and $\frac{16}{3}$ in the statement of Theorem 1 are not important. They can be improved by bootstrapping the analysis. After all, the condition $\left\| D^{-1} \Delta G^* \right\|_F \le \frac{\sqrt{n}}{32\rho}$ used to obtain inequality (7) is only a very weak requirement for the conclusion of Theorem 1 to hold and may not reflect the true magnitude of $\left\| D^{-1} \Delta G^* \right\|_F$. The key message conveyed by Theorem 1 is that the estimation error of the iterates produced by the suitably initialized GPM decreases geometrically to some parameter characterized by the measurement graph and the noise.

4.1 Proof of Theorem 1

The proof of Theorem 1 requires the following Lemma 2 which asserts that the projection map Π satisfies a certain contraction-type property and is a generalization of [29, Proposition 3.3] from $\mathcal{SO}(2)$ to arbitrary closed subgroups of the orthogonal group. Since [29, Proposition 3.3] has already been applied in a number of works to study phase synchronization problems [49] or even other estimation problems [18, 44], we believe that Lemma 2 will find further applications in synchronization problems or other estimation or optimization problems over general subgroups of the orthogonal group. Furthermore, the proof of Lemma 2 is different from and much simpler than that of [29, Proposition 3.3].

Lemma 2. *For any $r > 0$, $X \in \mathbb{R}^{d\times d}$ and $Q \in \mathcal{G}$,*

$$\|\Pi(X) - Q\|_F \le 2\left\|r^{-1}X - Q\right\|_F.$$

Proof. Using Lemma 1 and the definition of Π, we have

$$\begin{aligned}
&\|\Pi(X) - Q\|_F = \left\|\Pi\left(r^{-1}X\right) - Q\right\|_F \\
\le &\left\|\Pi\left(r^{-1}X\right) - r^{-1}X\right\|_F + \left\|r^{-1}X - Q\right\|_F \\
\le &\left\|Q - r^{-1}X\right\|_F + \left\|r^{-1}X - Q\right\|_F \\
= &\,2\left\|r^{-1}X - Q\right\|_F,
\end{aligned}$$

which completes the proof. □

The proof of Theorem 1 also relies on the following technical lemma.

Lemma 3. *Let $\rho \ge 1$. If for some $t \ge 0$,*

$$\left\|G^{*\top}G^t - n\cdot Q^t\right\|_F \le \rho\cdot \operatorname{Tr}\left(n\cdot I_d - Q^{t\top}G^{*\top}G^t\right),$$

then

$$\epsilon(G^{t+1}) \le 2\left(\frac{\rho\cdot\epsilon(G^t)}{2\sqrt{n}} + \sqrt{\kappa} + \left\|D^{-1}\Delta\right\|\right)\epsilon(G^t) + 2\left\|D^{-1}\Delta G^*\right\|_F.$$

Proof. Using Lemma 2 and the fact that $G_i^*Q^t \in \mathcal{G}$, we have that for any $t = 1, 2\ldots$, and $i = 1,\ldots,n$,

$$\left\|\Pi\left(\left[CG^t\right]_i\right) - G_i^*Q^t\right\|_F \le 2\left\|\left[r_i^{-1}\cdot CG^t\right]_i - G_i^*Q^t\right\|_F. \tag{8}$$

Then, we have

$$\begin{aligned}
&\epsilon(G^{t+1}) = \min_{Q\in\mathcal{G}}\|G^{t+1} - G^*Q\|_F \le \|G^{k+1} - G^*Q^t\|_F = \|\Pi^n\left(CG^t\right) - G^*Q^t\|_F \\
\le &\,2\left\|D^{-1}CG^t - G^*Q^t\right\|_F \le 2\left\|D^{-1}(C-\Delta)G^t - G^*Q^t\right\|_F + 2\left\|D^{-1}\Delta G^t\right\|_F \\
\le &\,2\left\|D^{-1}(C-\Delta)G^t - G^*Q^t\right\|_F + 2\left\|D^{-1}\Delta(G^t - G^*Q^t)\right\|_F + 2\left\|D^{-1}\Delta G^*Q^t\right\|_F \\
\le &\,2\left\|D^{-1}(C-\Delta)G^t - G^*Q^t\right\|_F + 2\left\|D^{-1}\Delta\right\|\cdot\epsilon(G^t) + 2\left\|D^{-1}\Delta G^*\right\|_F,
\end{aligned} \tag{9}$$

where the second inequality follows from inequality (8). Using the definitions of C, Δ and μ_{jk}, we have that

$$
\begin{aligned}
&\left\|D^{-1}(C-\Delta)G^t - G^*Q^t\right\|_F^2 = \sum_{i=1}^n \left\|\left[D^{-1}(C-\Delta)G^t - G^*Q^t\right]_i\right\|_F^2 \\
&= \sum_{i=1}^n \left\| \frac{1}{r_i}\sum_{j=1}^n [C-\Delta]_{ij}\,[G^t]_j - G_i^*Q^t \right\|_F^2 = \sum_{i=1}^n \left\| \frac{1}{r_i}\sum_{j=1}^n w_{ij}\cdot G_i^* G_j^{*\top}\,[G^t]_j - G_i^*Q^t \right\|_F^2 \\
&= \sum_{i=1}^n \left\| \frac{1}{r_i}\sum_{j=1}^n w_{ij}\cdot G_j^{*\top}\,[G^t]_j - Q^t \right\|_F^2 = \sum_{j=1}^n\sum_{k=1}^n \mu_{jk}\cdot \left\langle G_j^{*\top}[G^t]_j - Q^t, G_k^{*\top}[G^t]_k - Q^t \right\rangle \\
&= \frac{1}{n}\cdot\left\langle \sum_{j=1}^n \left(G_j^{*\top}[G^t]_j - Q^t\right), \sum_{k=1}^n \left(G_k^{*\top}[G^t]_k - Q^t\right)\right\rangle \\
&\qquad + \sum_{j\neq k}\left(\mu_{jk} - \frac{1}{n}\right)\left\langle G_j^{*\top}[G^t]_j - Q^t, G_k^{*\top}[G^t]_k - Q^t \right\rangle \\
&\qquad + \sum_{j=1}^n\left(\mu_{jj} - \frac{1}{n}\right)\left\langle G_j^{*\top}[G^t]_j - Q^t, G_j^{*\top}[G^t]_j - Q^t \right\rangle .
\end{aligned}
\tag{10}
$$

We handle the terms in the last line of equation (10) separately. The first term in the last line of (10) can be bounded as

$$
\begin{aligned}
&\frac{1}{n}\cdot\left\langle \sum_{j=1}^n \left(G_j^{*\top}[G^t]_j - Q^t\right), \sum_{k=1}^n \left(G_k^{*\top}[G^t]_k - Q^t\right)\right\rangle \\
&= \frac{1}{n}\left\langle G^{*\top}G^t - n\cdot Q^t, G^{*\top}G^t - n\cdot Q^t\right\rangle = \frac{1}{n}\cdot\left\|G^{*\top}G^t - n\cdot Q^t\right\|_F^2 \\
&\le \frac{\rho^2}{n}\cdot\left(\mathrm{Tr}\left(n\cdot I_d - {Q^t}^\top G^{*\top}G^t\right)\right)^2 = \frac{\rho^2}{4n}\cdot\left(\left\|G^t\right\|_F^2 - 2\left\langle G^t, G^*Q^t\right\rangle + \left\|G^*Q^t\right\|_F^2\right)^2 \\
&= \frac{\rho^2}{4n}\left\|G^t - G^*Q^t\right\|_F^4 = \frac{\rho^2}{4n}\cdot\left(\epsilon(G^t)\right)^4 ,
\end{aligned}
\tag{11}
$$

where the inequality follows from the supposition. The second and third terms in the last line of (10) can be bounded as

$$
\begin{aligned}
&\sum_{j\neq k}\left(\mu_{jk}-\frac{1}{n}\right)\left\langle G_j^{*\top}[G^t]_j-Q^t, G_k^{*\top}[G^t]_k-Q^t\right\rangle \\
&\qquad+\sum_{j=1}^{n}\left(\mu_{jj}-\frac{1}{n}\right)\left\langle G_j^{*\top}[G^t]_j-Q^t, G_j^{*\top}[G^t]_j-Q^t\right\rangle \\
&\leq \frac{\kappa_1}{n}\sum_{j,k}\left\|G_j^{*\top}[G^t]_j-Q^t\right\|_F\left\|G_k^{*\top}[G^t]_k-Q^t\right\|_F+\kappa_2\sum_{j=1}^{n}\left\|G_j^{*\top}[G^t]_j-Q^t\right\|_F^2 \\
&=(\kappa_1+\kappa_2)\sum_{j=1}^{n}\left\|G_j^{*\top}[G^t]_j-Q^t\right\|_F^2=\kappa\cdot\left\|G^t-G^*Q^t\right\|_F^2=\kappa\cdot\left(\epsilon(G^t)\right)^2,
\end{aligned}
\tag{12}
$$

where the first inequality follows from the definitions of κ_1 and κ_2 and the Cauchy-Schwarz inequality. Substituting (12) and (11) into (10), we get

$$
\left\|D^{-1}(C-\Delta)G^t-G^*Q^t\right\|_F\leq\sqrt{\frac{\rho^2}{4n}\cdot(\epsilon(G^t))^4+\kappa\cdot(\epsilon(G^t))^2}\leq\frac{\rho\cdot(\epsilon(G^t))^2}{2\sqrt{n}}+\sqrt{\kappa}\cdot\epsilon(G^t),
$$

which, combined with (9), yields the desired inequality. $\square$

Armed with Lemma 3, we can now prove the master theorem.

Proof of Theorem 1. We first show by induction that

$$
\epsilon(G^t)\leq\frac{\sqrt{n}}{2\rho}\quad\forall t\geq 0. \tag{13}
$$

For $t=0$, it follows from the supposition that $\epsilon(G^0)\leq\frac{\sqrt{n}}{2\rho}$. Next, we assume that $\epsilon(G^t)\leq\frac{\sqrt{n}}{2\rho}$ for some $t\geq 0$. Then, by Lemma 3, conditions (ii)-(iii) and the induction hypothesis, we have that

$$
\begin{aligned}
\epsilon(G^{t+1})&\leq 2\left(\frac{\rho\cdot\epsilon(G^t)}{2\sqrt{n}}+\sqrt{\kappa}+\left\|D^{-1}\Delta\right\|\right)\epsilon(G^t)+2\left\|D^{-1}\Delta G^*\right\|_F \\
&\leq 2\left(\frac{1}{4}+\frac{1}{32}+\frac{1}{32}\right)\frac{\sqrt{n}}{2\rho}+\frac{\sqrt{n}}{16\rho}<\frac{\sqrt{n}}{2\rho},
\end{aligned}
$$

which yields inequality (13). Using Lemma 3, conditions (ii)-(iii) and inequality (13), we have that

$$
\begin{aligned}
\epsilon(G^{t+1}) &\le 2\left(\frac{\rho\cdot\epsilon(G^t)}{2\sqrt{n}} + \sqrt{\kappa} + \left\|D^{-1}\Delta\right\|\right)\epsilon(G^t) + 2\left\|D^{-1}\Delta G^*\right\|_F \\
&\le \frac{5}{8}\cdot\epsilon(G^t) + 2\left\|D^{-1}\Delta G^*\right\|_F \\
&\le \frac{5}{8}\cdot\left(\frac{5}{8}\cdot\epsilon(G^{t-1}) + 2\left\|D^{-1}\Delta G^*\right\|_F\right) + 2\left\|D^{-1}\Delta G^*\right\|_F \\
&= \left(\frac{5}{8}\right)^2\epsilon(G^{t-1}) + \left(1+\frac{5}{8}\right)2\left\|D^{-1}\Delta G^*\right\|_F \\
&\le \left(\frac{5}{8}\right)^{t+1}\epsilon(G^0) + \left(1+\frac{5}{8}+\left(\frac{5}{8}\right)^2\cdots\right)2\left\|D^{-1}\Delta G^*\right\|_F \\
&= \left(\frac{5}{8}\right)^{t+1}\epsilon(G^0) + \frac{16}{3}\left\|D^{-1}\Delta G^*\right\|_F,
\end{aligned}
$$

which completes the proof. □

We shall demonstrate the usefulness of Theorem 1 by studying concrete examples of the subgroup $\mathcal{G}$, the measurement graph and the noise model that are commonplace in applications of synchronization problems. Specifically, from Sections 5 to 8, we will show that the conditions (i) to (iv) of the theorem hold for these particular examples, thereby demonstrating that Theorem 1 encompasses a large class of synchronization problems in practice.

5 Four Specific Subgroups $\mathcal{G}$

Four specific subgroups $\mathcal{G}$, namely $\mathcal{O}(d)$, $\mathcal{SO}(d)$, $\mathcal{P}(d)$ and $\mathcal{Z}_m$, are considered in this section. We will show that the projection $\Pi_{\mathcal{G}}$ associated with these can be easily computed (in polynomial time) and that condition (i) holds for all of them. The main results of this section is summarized in the following theorem.

Theorem 2. *Let the group $\mathcal{G}$ be $\mathcal{O}(d)$, $\mathcal{SO}(d)$, $\mathcal{P}(d)$ or $\mathcal{Z}_m$ for $m \ge 1$. Also, let $\{G^t\}_{t\ge 1}$ be the iterates of GPM for $\mathcal{G}$-*sync *and Q^t be defined as in* (6)*. Then, there exists a constant $\rho \ge 1$ such that for any $t \ge 0$,*

$$
\left\|{G^*}^\top G^t - n\cdot Q^t\right\|_F \le \rho\,\mathrm{Tr}\left(n\cdot I_d - {Q^t}^\top {G^*}^\top G^t\right). \tag{14}
$$

In particular, $\rho = 1$ if $\mathcal{G}$ is $\mathcal{O}(d)$, $\mathcal{SO}(d)$, $\mathcal{P}(d)$ or $\mathcal{Z}_m$ for $m = 1, 2$; and $\rho = (\sin\pi/m)^{-1}$ if $\mathcal{G}$ is $\mathcal{Z}_m$ for $m \ge 3$. Furthermore, in the case of $\mathcal{O}(d)$ and $\mathcal{SO}(d)$, the projection $\Pi_{\mathcal{G}}$ can be computed in closed form via the singular value decomposition of a $d \times d$ matrix; in the *case of $\mathcal{P}(d)$, the projection $\Pi_{\mathcal{G}}$ can be computed via a d-dimensional linear programming problem; and in the case of $\mathcal{Z}_m$, the projection $\Pi_{\mathcal{G}}$ can be computed in closed form via some trigonometric function as in Proposition 1.*

We prove Theorem 2 for the groups $\mathcal{O}(d)$, $\mathcal{SO}(d)$, $\mathcal{P}(d)$ and $\mathcal{Z}_m$ in Sections 5.1, 5.2, 5.3, and 5.4 respectively.

Motivated by Theorem 2, the following conjecture is formulated.

Conjecture 1. *Let $\mathcal{G}$ be a closed subgroup of the orthogonal group $\mathcal{O}(d)$ and its convex hull be denoted by $conv(\mathcal{G})$. Then, there exists a constant $\rho \geq 1$ such that*

$$\operatorname{dist}(X, \mathcal{G}) \leq \rho \operatorname{Tr}(I_d - X^\top \Pi_{\mathcal{G}}(X)) \quad \forall X \in conv(\mathcal{G}). \tag{15}$$

The validity of Conjecture 1 would imply that condition (i) of the master theorem is superfluous and hence that the theoretical results of this paper apply to arbitrary closed subgroups of the orthogonal group. Indeed, by taking $X = \frac{1}{n} G^{*\top} G^t$, one readily verifies inequality (14) from inequality (15).

5.1 $\mathcal{O}(d)$-sync

The projection $\Pi_{\mathcal{O}(d)}$ is given by the well-known *orthogonal Procrustes problem* [21], *i.e.*, for any $X \in \mathbb{R}^{d \times d}$ with singular value decomposition $U_X \Sigma_X V_X^\top$, the projection is given by

$$\Pi_{\mathcal{O}(d)}(X) = U_X V_X^\top.$$

Next, we prove the Conjecture 1 for $\mathcal{O}(d)$. Since $X \in \operatorname{conv}(\mathcal{O}(d))$, by the Carathéodory's theorem, there exist $Q_1, \ldots, Q_L \in \mathcal{O}(d)$ and $\alpha_1, \ldots, \alpha_L \geq 0$ such that

$$\sum_{\ell=1}^{L} \alpha_\ell = 1 \quad \text{and} \quad X = \sum_{\ell=1}^{L} \alpha_\ell Q_\ell.$$

Then, for any $j = 1, \ldots, d$,

$$\sigma_j(X) = \sigma_j \left(\sum_{\ell=1}^{L} \alpha_\ell Q_\ell \right) \leq \sum_{\ell=1}^{L} \alpha_\ell \sigma_j (Q_\ell) = \sum_{\ell=1}^{L} \alpha_\ell = 1. \tag{16}$$

Using the above inequality, we have that $I_d - \Sigma_X$ is positive semidefinite and that

$$\begin{aligned} \operatorname{dist}(X, \mathcal{O}(d)) &= \left\| X - \Pi_{\mathcal{O}(d)}(X) \right\|_F = \left\| U_X \Sigma_X V_X^\top - U_X V_X^\top \right\|_F = \| I_d - \Sigma_X \|_F \\ &\leq \operatorname{Tr}(I_d - \Sigma_X) = \operatorname{Tr}\left(I_d - V_X \Sigma_X {V_X}^\top \right) = \operatorname{Tr}\left(I_d - X^\top \Pi_{\mathcal{O}(d)}(X) \right), \end{aligned}$$

which yields inequality (15) for $\mathcal{O}(d)$-sync.

5.2 $\mathcal{SO}(d)$-sync

We adopt a similar strategy to prove inequality (14) for $\mathcal{SO}(d)$-sync. To do so, we need an analytic expression for the projection operator $\Pi_{\mathcal{SO}(d)}$, which is given by the *Kabsch algorithm* [25].

Lemma 4. *Let $X \in \mathbb{R}^{d\times d}$ be a matrix with singular decomposition $X = U_X \Sigma_X V_X^\top$. Define*

$$I_X = \begin{pmatrix} 1 & & & \\ & \ddots & & \\ & & 1 & \\ & & & \det(U_X V_X^\top) \end{pmatrix} \in \mathbb{R}^{d\times d}.$$

Then

$$\Pi_{\mathcal{SO}(d)}(X) = U_X I_X V_X^\top.$$

We can now prove inequality (15) similarly to the case of $\mathcal{O}(d)$. Specifically, using Lemma 4, we have

$$\begin{aligned}\operatorname{dist}(X, \mathcal{SO}(d)) &= \left\|X - \Pi_{\mathcal{SO}(d)}(X)\right\|_F = \left\|U_X \Sigma_X V_X{}^\top - U_X I_X V_X{}^\top\right\|_F = \|I_d - \Sigma_X I_X\|_F \\ &\leq \operatorname{Tr}(I_d - \Sigma_X I_X) = \operatorname{Tr}\left(I_d - V_X \Sigma_X I_X V_X{}^\top\right) = \operatorname{Tr}\left(I_d - X^\top \Pi_{\mathcal{SO}(d)}(X)\right),\end{aligned}$$

where the inequality follows from (16). This shows that inequality (15) holds for $\mathcal{SO}(d)$-sync.

5.3 $\mathcal{P}(d)$-sync

Given any $X \in \mathbb{R}^{d\times d}$, the projection $\Pi_{\mathcal{P}(d)}(X)$ is given by an optimal solution of the *assignment problem* [12]:

$$\max_{Q\in\mathcal{P}(d)} \langle Q, X\rangle,$$

which can be solved in polynomial time by linear programming or the Hungarian algorithm, also known as the Kuhn–Munkres algorithm.

To prove the inequality (15) for $\mathcal{P}(d)$, we first note that for any permutation matrix $P \in \mathcal{P}(d)$, either $d = \operatorname{Tr}(P)$ or $d - \operatorname{Tr}(P) \geq 2$. Then,

$$\begin{aligned}\|I_d - P\|_F^2 &= \sum_{i=1}^d \sum_{j=1}^d (I_d - P)_{ij}^2 = \sum_{i=1}^d \sum_{j=1}^d |(I_d - P)_{ij}| \\ &= \sum_{i\neq j} P_{ij} + \sum_{i=1}^d (1 - P_{ii}) = 2d - 2\operatorname{Tr}(P) \leq (d - \operatorname{Tr}(P))^2.\end{aligned} \tag{17}$$

For any $Y \in \operatorname{conv}(\mathcal{P}(d))$, by the Carathéodory's theorem, there exist $P_1, \ldots, P_L \in \mathcal{P}(d)$ and $\alpha_1, \ldots, \alpha_L \geq 0$ such that

$$\sum_{\ell=1}^{L} \alpha_\ell = 1 \quad \text{and} \quad Y = \sum_{\ell=1}^{L} \alpha_\ell P_\ell.$$

By inequality (17), we have that

$$\|I_d - Y\|_F \leq \sum_{\ell=1}^{L} \alpha_\ell \|I_d - P_\ell\|_F \leq \sum_{\ell=1}^{L} \alpha_\ell \left(d - \operatorname{Tr}\left(P_\ell\right)\right) = d - \operatorname{Tr}(Y). \tag{18}$$

Let $X \in \operatorname{conv}(\mathcal{P}(d))$. Then, $\Pi_{\mathcal{P}(d)}(X)^\top X \in \operatorname{conv}(\mathcal{P}(d))$. Using inequality (18) with $Y = \Pi_{\mathcal{P}(d)}(X)^\top X$, we obtain

$$\begin{aligned}\operatorname{dist}(X, \mathcal{P}(d)) &= \left\|X - \Pi_{\mathcal{P}(d)}(X)\right\|_F = \left\|\Pi_{\mathcal{P}(d)}(X)^\top X - I_d\right\|_F \\ &\leq d - \operatorname{Tr}\left(\Pi_{\mathcal{P}(d)}(X)^\top X\right) = \operatorname{Tr}\left(I_d - X^\top \Pi_{\mathcal{P}(d)}(X)\right),\end{aligned}$$

which yields inequality (15) for $\mathcal{P}(d)$-sync.

5.4 $\mathcal{Z}_m$-sync

We first prove that Conjecture 1 holds for $\mathcal{Z}_m$ for any positive integer m. In particular, we will show that

$$\operatorname{dist}(X, \mathcal{Z}_m) \leq \begin{cases} \operatorname{Tr}\left(I_d - X^\top \Pi_{\mathcal{G}}(X)\right) & \text{if } m = 1, 2, \\ \frac{1}{\sqrt{2}\sin\left(\frac{\pi}{m}\right)} \operatorname{Tr}\left(I_d - X^\top \Pi_{\mathcal{G}}(X)\right) & \text{if } m \geq 3. \end{cases}$$

To do so, we note that for any $X \in \operatorname{conv}(\mathcal{Z}_m)$, X is of the form

$$X = \begin{pmatrix} x & -y \\ y & x \end{pmatrix}.$$

For any 2×2 matrix of the above form, we let $z_X \in \mathbb{C}$ be the complex number $z_X = x + \mathbf{i}y$, where $\mathbf{i}$ is the imaginary unit. Let $\Re(z)$ be the real part of any complex number $z \in \mathbb{C}$,

$$Q_k = \begin{pmatrix} \cos\frac{2k\pi}{m} & -\sin\frac{2k\pi}{m} \\ \sin\frac{2k\pi}{m} & \cos\frac{2k\pi}{m} \end{pmatrix}, \quad k = 0, \ldots, m-1, \tag{19}$$

and

$$\hat{k}(X) \in \operatorname*{argmin}_{k=0,\ldots,m-1} \|X - Q_k\|_F^2.$$

For $m = 1$, $\hat{k}(X) = 0$ for any $X \in \mathrm{conv}(\mathcal{Z}_1)$ and hence $\Pi_{\mathcal{Z}_1}(X) = Q_0 = I_2$. It follows that

$$\mathrm{dist}(X, \mathcal{Z}_1) = \|X - I_2\|_F \leq \mathrm{Tr}(I_2 - X) = \mathrm{Tr}(I_2 - X^\top \Pi_{\mathcal{Z}_1}(X)),$$

which yields the desired inequality (15). For $m = 2$, if $\Re(z_X) = x \geq 0$, then $\hat{k}(X) = 0$ and $\Pi_{\mathcal{Z}_1}(X) = Q_0 = I_2$; if $\Re(z_X) = x < 0$, then $\hat{k}(X) = 1$ and $\Pi_{\mathcal{Z}_1}(X) = Q_1 = -I_2$. Therefore,

$$\mathrm{dist}(X, \mathcal{Z}_2) = \begin{cases} \|X - I_2\|_F \\ \|X + I_2\|_F \end{cases} \leq \begin{cases} \mathrm{Tr}(I_2 - X) \\ \mathrm{Tr}(I_2 + X) \end{cases} \leq \begin{cases} \mathrm{Tr}(I_2 - X^\top \Pi_{\mathcal{Z}_1}(X)) & \text{if } x \geq 0, \\ \mathrm{Tr}(I_2 - X^\top \Pi_{\mathcal{Z}_1}(X)) & \text{if } x < 0, \end{cases}$$

which yields the desired inequality (15).

Now we assume $m \geq 3$. We have that

$$\mathrm{dist}(X, \mathcal{Z}_m) = \left\|X - Q_{\hat{k}(X)}\right\|_F = \sqrt{2}\left|z_X - z_{Q_{\hat{k}(X)}}\right| = \sqrt{2}\left|z_X - e^{\frac{2\hat{k}(X)\pi \mathbf{i}}{m}}\right|, \tag{20}$$

where $|\cdot|$ denotes the modulus of complex numbers. On the other hand,

$$\mathrm{Tr}\left(I_2 - X^\top \Pi_{\mathcal{Z}_m}(X)\right) = 2 - \mathrm{Tr}(X^\top Q_{\hat{k}(X)}) = 2\left(1 - \Re\left(z_X \cdot e^{-\frac{2\hat{k}(X)\pi \mathbf{i}}{m}}\right)\right). \tag{21}$$

Therefore, we would like to upper bound the ratio

$$\frac{\left|z - e^{\frac{2k\pi \mathbf{i}}{m}}\right|}{\left(1 - \Re\left(z \cdot e^{-\frac{2k\pi \mathbf{i}}{m}}\right)\right)} \tag{22}$$

subject to the constraint that $z = z_X$ for some $X \in \mathrm{conv}(\mathcal{G})$ with $\hat{k}(X) = k$. By symmetry, we can assume without loss of generality that $\hat{k}(X) = 0$ and consider the shaded region $\mathcal{R}_0$ shown in Figure 1(a), which is defined as

$$\mathcal{R}_0 = \left\{z \in \mathbb{C} : z \in \mathrm{conv}(\mathcal{G}),\ 0 \in \underset{k=0,\ldots,m-1}{\mathrm{argmin}} \left|z - e^{\frac{2k\pi \mathbf{i}}{m}}\right|\right\}.$$

Over the region $\mathcal{R}_0$, the ratio (22) reduces to

$$\frac{|1 - z|}{(1 - \Re(z))}. \tag{23}$$

Let z_1 and z_2 be the midpoints between 1 and its two neighboring group elements $e^{2\pi \mathbf{i}/m}$ and $e^{-2\pi \mathbf{i}/m}$, respectively. We claim that any point in the line segments $[1, z_1] \cup [1, z_2]$ (see Figure 1(a)) is a maximizer of the ratio (23) over $\mathcal{R}_0$. To see this, we consider the polar representation $z' = |z'| \cdot e^{\mathbf{i}\phi}$ of the transformed variable $z' = 1 - z$, which lies in

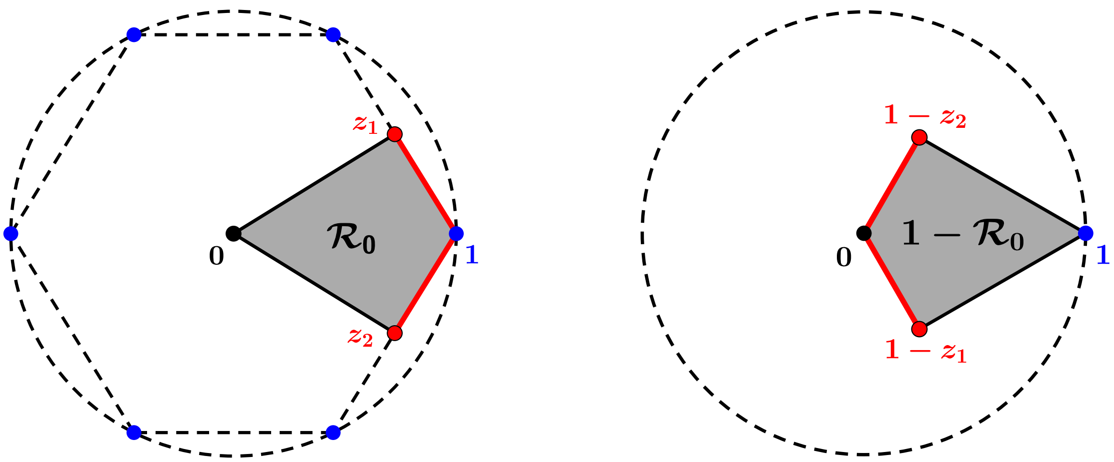

(a) $\mathcal{R}_0$ (b) $1 - \mathcal{R}_0$

Figure 1: Regions $\mathcal{R}_0$ and $1 - \mathcal{R}_0$. In Figure (a), blue points are the group elements of the cyclic group $\mathcal{Z}_m$; while points on the two red line segments are the maximizers of the ratio (23).

the region $1 - \mathcal{R}_0$ (see Figure 1(b)). By the angle sum formula for the regular m-gon, $\phi \in [-\pi(\frac{1}{2} - \frac{1}{m}), \pi(\frac{1}{2} - \frac{1}{m})]$. Then,

$$\begin{aligned} \max_{z \in \mathcal{R}_0} \frac{|1 - z|}{(1 - \Re(z))} &= \max_{z' \in 1 - \mathcal{R}_0} \frac{|z'|}{\Re(z')} = \max_{\phi \in [-\pi(\frac{1}{2} - \frac{1}{m}), \pi(\frac{1}{2} - \frac{1}{m})]} \frac{1}{\Re(e^{\mathbf{i}\phi})} \\ &= \max_{\phi \in [-\pi(\frac{1}{2} - \frac{1}{m}), \pi(\frac{1}{2} - \frac{1}{m})]} \frac{1}{\cos \phi} \leq \frac{1}{\cos(\pi(\frac{1}{2} - \frac{1}{m}))} = \frac{1}{\sin\left(\frac{\pi}{m}\right)}. \end{aligned} \tag{24}$$

This proves the claim since

$$\frac{|1 - z|}{(1 - \Re(z))} = \frac{1}{\sin\left(\frac{\pi}{m}\right)} \quad \forall z \in [1, z_1] \cup [1, z_2].$$

Using (20), (21) and (24), we get

$$\operatorname{dist}(X, \mathcal{Z}_m) \leq \frac{1}{\sqrt{2} \sin\left(\frac{\pi}{m}\right)} \operatorname{Tr}\left(I_d - X^\top \Pi_{\mathcal{G}}(X)\right),$$

which shows that Conjecture 1 holds for $\mathcal{G} = \mathcal{Z}_m$.

Next, we derive an explicit formula for computing projections onto the group $\mathcal{Z}_m$.

Proposition 1. *For any*

$$X = \begin{pmatrix} x_{11} & x_{12} \\ x_{21} & x_{22} \end{pmatrix} \in \mathbb{R}^{2 \times 2},$$

not necessarily in $\operatorname{conv}(\mathcal{G})$, *define*

$$\theta = \begin{cases} \arccos \frac{x_{21}-x_{12}}{\sqrt{(x_{11}+x_{22})^2+(x_{21}-x_{12})^2}} & \text{if } x_{11}+x_{22} \geq 0, \\ 2\pi - \arccos \frac{x_{21}-x_{12}}{\sqrt{(x_{11}+x_{22})^2+(x_{21}-x_{12})^2}} & \text{if } x_{11}+x_{22} < 0, \end{cases}$$

which always lies in $[0, 2\pi)$. *Then, for any* $m \geq 1$,

$$\Pi_{\mathcal{Z}_m}(X) = \begin{cases} Q_{round(\frac{m}{4}-\frac{m\theta}{2\pi})} & \text{if } 0 \leq \theta \leq \frac{\pi}{2}+\frac{\pi}{m}, \\ Q_{round(\frac{5m}{4}-\frac{m\theta}{2\pi})} & \text{if } \frac{\pi}{2}+\frac{\pi}{m} < \theta < 2\pi, \end{cases}$$

where $round(\,\cdot\,)$ *rounds a number to its closest integer and* Q_k *is defined in* (19).

Proof. The case of $m = 1$ is trivial. We assume that $m \geq 2$. Then,

$$\begin{aligned} \operatorname*{argmin}_{k=0,\dots,m-1} \|X - Q_k\|_F^2 &= \operatorname*{argmin}_{k=0,\dots,m-1} \langle X, Q_k \rangle \\ &= \operatorname*{argmin}_{k=0,\dots,m-1} (x_{11}+x_{22}) \cos \frac{2k\pi}{m} + (x_{21}-x_{12}) \sin \frac{2k\pi}{m} \\ &= \operatorname*{argmin}_{k=0,\dots,m-1} \sin\left(\theta + \frac{2k\pi}{m}\right). \end{aligned} \tag{25}$$

Since θ can take any value in $[0, 2\pi)$ and $\frac{2k\pi}{m}$ lies inside $[0, \frac{2(m-1)\pi}{m}]$, we have that

$$0 \leq \theta + \frac{2k\pi}{m} \leq 2\pi + \frac{2(m-1)\pi}{m} < 4\pi.$$

There are two peaks of the function $\sin(\cdot)$ on $[0, 2\pi + \frac{2(m-1)\pi}{m})$: $\frac{\pi}{2}$ and $\frac{5\pi}{2}$. By the above observation and (25), we have that

$$\operatorname*{argmin}_{k=0,\dots,m-1} \|X - Q_k\|_F^2 = \operatorname*{argmin}_{k=0,\dots,m-1} \min\left\{\left|\theta + \frac{2k\pi}{m} - \frac{\pi}{2}\right|, \left|\theta + \frac{2k\pi}{m} - \frac{5\pi}{2}\right|\right\}. \tag{26}$$

We first consider the case $0 \leq \theta \leq \frac{\pi}{2} + \frac{\pi}{m}$. Then,

$$\theta + \frac{2k\pi}{m} \leq \frac{\pi}{2} + \frac{\pi}{m} + \frac{2(m-1)\pi}{m} = \frac{5\pi}{2} - \frac{\pi}{m},$$

which implies that

$$\left|\theta + \frac{2k\pi}{m} - \frac{5\pi}{2}\right| \geq \frac{\pi}{m}.$$

Also, since

$$\frac{m}{4} - \frac{m\theta}{2\pi} \geq \frac{m}{4} - \frac{m}{2\pi}\left(\frac{\pi}{2} + \frac{\pi}{m}\right) = -\frac{1}{2},$$

we have $\mathrm{round}(\frac{m}{4} - \frac{m\theta}{2\pi}) \in \{0, \ldots, m-1\}$. Setting $k = \mathrm{round}(\frac{m}{4} - \frac{m\theta}{2\pi})$, then

$$\left| k - \left(\frac{m}{4} - \frac{m\theta}{2\pi} \right) \right| \leq \frac{1}{2},$$

and hence

$$\left| \theta + \frac{2k\pi}{m} - \frac{\pi}{2} \right| \leq \frac{\pi}{m}.$$

By (26),

$$\begin{aligned} \operatorname*{argmin}_{k=0,\ldots,m-1} \|X - Q_k\|_F^2 &= \operatorname*{argmin}_{k=0,\ldots,m-1} \left| \theta + \frac{2k\pi}{m} - \frac{\pi}{2} \right| \\ &= \operatorname*{argmin}_{k=0,\ldots,m-1} \left| k - \left(\frac{m}{4} - \frac{m\theta}{2\pi} \right) \right| = \mathrm{round}\left(\frac{m}{4} - \frac{m\theta}{2\pi} \right). \end{aligned}$$

Next, we consider the case $\frac{\pi}{2} + \frac{\pi}{m} < \theta < 2\pi$. Then,

$$\theta + \frac{2k\pi}{m} - \frac{\pi}{2} > \frac{\pi}{2} + \frac{\pi}{m} - \frac{\pi}{2} = \frac{\pi}{m},$$

which implies that

$$\left| \theta + \frac{2k\pi}{m} - \frac{\pi}{2} \right| \geq \frac{\pi}{m}.$$

Also, since

$$\frac{5m}{4} - \frac{m\theta}{2\pi} < \frac{5m}{4} - \frac{m}{2\pi}\left(\frac{\pi}{2} + \frac{\pi}{m} \right) = m - \frac{1}{2},$$

we have $\mathrm{round}(\frac{5m}{4} - \frac{m\theta}{2\pi}) \in \{0, \ldots, m-1\}$. Setting $k = \mathrm{round}(\frac{5m}{4} - \frac{m\theta}{2\pi})$, then

$$\left| k - \left(\frac{5m}{4} - \frac{m\theta}{2\pi} \right) \right| \leq \frac{1}{2},$$

and hence

$$\left| \theta + \frac{2k\pi}{m} - \frac{5\pi}{2} \right| \leq \frac{\pi}{m}.$$

By (26),

$$\begin{aligned} \operatorname*{argmin}_{k=0,\ldots,m-1} \|X - Q_k\|_F^2 &= \operatorname*{argmin}_{k=0,\ldots,m-1} \left| \theta + \frac{2k\pi}{m} - \frac{5\pi}{2} \right| \\ &= \operatorname*{argmin}_{k=0,\ldots,m-1} \left| k - \left(\frac{5m}{4} - \frac{m\theta}{2\pi} \right) \right| = \mathrm{round}\left(\frac{5m}{4} - \frac{m\theta}{2\pi} \right). \end{aligned}$$

This completes the proof. $\square$

6 The Erdös-Rényi Measurement Graphs

We verify condition (ii) for a random graph model for the measurement graphs $([n], E)$: the *Erdös-Rényi graphs.* More precisely, recall that $\{w_{ij}\}_{i<j}$ are the upper-triangular entries of the adjacency matrix of the extended measurement graph $([n], \bar{E})$. If $\{w_{ij}\}_{i<j}$ are random variables distributed independently and identically as

$$w_{ij} = \begin{cases} 1 & \text{with probability } p, \\ 0 & \text{with probability } 1-p, \end{cases} \qquad \text{for } i < j,$$

then the measurement graph of the synchronization problem is said to be Erdös-Rényi. The parameter $p \in (0,1)$ is called the *observation rate.* The following result asserts that condition (ii) of the master theorem holds for such a measurement graph with overwhelming probability.

Theorem 3. *Suppose that the synchronization problem has an Erdös-Rényi measurement graph with observation rate p. Then, there exist numerical constants $c_1, c_2, c_3 \in (0,1)$ and $c_4 > 0$ such that if $p \geq \frac{c_4}{n}$, we have*

$$\kappa \leq \frac{1}{1024},$$

with probability at least

$$1 - 2n \exp\left(-2c_1^2 np^2 + 4c_1 p\right) - n(n-1)\exp\left(-\frac{c_2^2}{4} np^2 + c_2\right) - n \exp\left(-2c_3^2 np^2 + 4c_3 p\right).$$

Proof. Recall that

$$r_i = \sum_{\ell=1}^{n} w_{i\ell}, \quad \mu_{jk} = \sum_{i=1}^{n} \frac{w_{ij} w_{ik}}{r_i^2}, \quad \kappa_1 = n \cdot \max_{j \neq k} \left| \mu_{jk} - \frac{1}{n} \right| \quad \text{and} \quad \kappa_2 = \max_j \left(\mu_{jj} - \frac{1}{n} \right),$$

where $w_{ij} = w_{ji}$ for $i > j$; and $w_{ii} = 1$ for all $i = 1, \ldots, n$. We first note that there exist numerical constants $c_1, c_2, c_3 \in (0,1), c_4 > 0$ such that

$$1 - \frac{1}{2048} \leq \frac{1 - c_2}{(1+c_1)^2} \quad \text{and} \quad \frac{1+c_2}{(1-c_1)^2} \leq 1 + \frac{1}{2048}, \tag{27}$$

and that for $p \in [\frac{c_4}{n}, 1]$,

$$\frac{1+c_3}{pn(1-c_1)^2} \leq \frac{1+c_3}{c_4(1-c_1)^2} \leq \frac{1}{2048} \leq \frac{1}{n} + \frac{1}{2048}. \tag{28}$$

Using the definitions of $\kappa, \kappa_1, \kappa_2$ and inequalities (27) and (28), we have

$$\begin{aligned}
&\Pr\left(\kappa \le \frac{1}{1024}\right) \ge \Pr\left(\kappa_1 \le \frac{1}{2048} \quad \text{and} \quad \kappa_2 \le \frac{1}{2048}\right) \\
&= \Pr\left(\frac{1}{n}\left(1 - \frac{1}{2048}\right) \le \mu_{jk} \le \frac{1}{n}\left(1 + \frac{1}{2048}\right) \ \forall j < k, \text{ and } \mu_{jj} \le \frac{1}{n} + \frac{1}{2048} \ \forall j \in [n]\right) \\
&\ge \Pr\left(\frac{1}{n} \cdot \frac{1 - c_2}{(1 + c_1)^2} \le \mu_{jk} \le \frac{1}{n} \cdot \frac{1 + c_2}{(1 - c_1)^2} \ \forall j < k, \text{ and } \mu_{jj} \le \frac{1 + c_3}{pn(1 - c_1)^2} \ \forall j \in [n]\right).
\end{aligned} \tag{29}$$

To bound the last probability, we define the random variable

$$b_{jk} := \sum_{i=1}^{n} w_{ij} w_{ik}.$$

By the definition of w_{ij},

$$r_i = 1 + \sum_{\ell \ne i} w_{i\ell} \quad \text{and} \quad b_{jk} = \begin{cases} 2w_{jk} + \sum_{i \ne j,k} w_{ij} w_{ik} & \text{if } j \ne k, \\ 1 + \sum_{i \ne j} w_{ij}^2 & \text{if } j = k. \end{cases}$$

We first bound r_i. For any $s_1 \in (0, 1)$, we have

$$\begin{aligned}
\Pr\left(np(1 - s_1) \le r_i \le np(1 + s_1)\right) &\ge \Pr\left(np(1 - s_1) \le \sum_{\ell \ne i} w_{i\ell} \le np(1 + s_1) - 1\right) \\
&\ge \Pr\left(\left|\sum_{\ell \ne i} w_{i\ell} - (n - 1)p\right| \le s_1 np - 1\right) \\
&\ge 1 - 2\exp\left(-2s_1^2 np^2 + 4s_1 p\right),
\end{aligned} \tag{30}$$

where the last inequality follows from the Hoeffding's inequality. Next, we bound b_{jk} for $j < k$. For any $i \in [n] \setminus \{j, k\}$, the random variable $w_{ij} w_{ik} - p^2$ satisfies that

$$|w_{ij} w_{ik} - p^2| \le 1, \quad \mathbb{E}[w_{ij} w_{ik} - p^2] = 0 \quad \text{and} \quad \mathbb{E}[(w_{ij} w_{ik} - p^2)^2] \le p^2.$$

By Bernstein inequality, for any $s_2 \in (0, 1)$, we have that

$$\begin{aligned}
\Pr\left(\left|\sum_{i \ne j,k} w_{ij} w_{ik} - (n - 2)p^2\right| > s_2 np^2 - 2\right) &\le 2\exp\left(\frac{-\frac{1}{2}(s_2 np^2 - 2)^2}{(n - 2)p^2 + \frac{1}{3}(s_2 np^2 - 2)}\right) \\
&\le 2\exp\left(-\frac{s_2^2 np^2 - 4s_2}{2(1 + \frac{s_2}{3})}\right) \\
&\le 2\exp\left(-\tfrac{s_2^2}{4} np^2 + s_2\right),
\end{aligned}$$

which implies that

$$
\begin{aligned}
& \Pr\left(np^2(1-s_2) \le b_{jk} \le np^2(1+s_2)\right) \\
\ge\ & \Pr\left(np^2(1-s_2) \le \sum_{i\ne j,k} w_{ij}w_{ik} \le np^2(1+s_2) - 2\right) \\
\ge\ & \Pr\left(\left|\sum_{i\ne j,k} w_{ij}w_{ik} - (n-2)p^2\right| \le s_2 np^2 - 2\right) \\
\ge\ & 1 - 2\exp\left(-\tfrac{s_2^2}{4}np^2 + s_2\right).
\end{aligned}
\tag{31}
$$

For b_{jj}, since w_{ij} is a Bernoulli random variable, b_{jj} has the same distribution as r_j. Therefore, for any $s_3 \in (0,1)$, we have

$$
\Pr\left(np(1-s_3) \le b_{jj} \le np(1+s_3)\right) \ge 1 - 2\exp\left(-2s_3^2np^2 + 4s_3p\right). \tag{32}
$$

Finally, substituting the definition of μ_{jk} into (29), we get

$$
\begin{aligned}
& \Pr\left(\kappa \le \frac{1}{1024}\right) \\
\ge\ & \Pr\left(\frac{np^2(1-c_2)}{n^2p^2(1+c_1)^2} \le \sum_{i=1}^{n} \frac{w_{ij}w_{ik}}{r_i^2} \le \frac{np^2(1+c_2)}{n^2p^2(1-c_1)^2}\ \forall j<k,\right. \\
& \qquad \left. \text{and} \quad \sum_{i=1}^{n} \frac{w_{ij}^2}{r_i^2} \le \frac{np(1+c_3)}{n^2p^2(1-c_1)^2}\ \forall j \in [n]\right) \\
\ge\ & \Pr\Big(np(1-c_1) \le r_i \le np(1+c_1)\ \forall i \in [n], \quad \text{and} \quad b_{jj} \le np(1+c_3)\ \forall j \in [n], \\
& \qquad \text{and} \quad np^2(1-c_2) \le b_{jk} \le np^2(1+c_2)\ \forall j<k\Big) \\
\ge\ & 1 - 2n\exp\left(-2c_1^2np^2 + 4c_1p\right) - n(n-1)\exp\left(-\tfrac{c_2^2}{4}np^2 + c_2\right) - n\exp\left(-2c_3^2np^2 + 4c_3p\right),
\end{aligned}
$$

where the last inequality follows from (30), (31), (32) and union bounds. This completes the proof. □

Although the proof of Theorem 3 requires only $p \ge \frac{c_4}{n}$, in order for the conclusion of the theorem to be non-trivial, the probability has to be positive, which in turn requires $p \ge \frac{c}{n^{1/2}}$ for some constant $c > 0$.

7 Additive Sub-Gaussian Noise

Recall that the measurements are given by

$$C_{ij} = G_i^* G_j^{*\top} + \Theta_{ij}, \quad (i,j) \in E.$$

The purpose of this section is to show that condition (iii) of Theorem 1 holds for a large and useful class of noise $\{\Theta_{ij}\}_{(i,j)\in E}$. Specifically, we focus on the case where each noise matrix Θ_{ij} is a random matrix with entries given by i.i.d. *sub-Gaussian* random variables.

Definition 1 (Sub-Gaussian Random Variable)**.** *A random variable ξ is said to be sub-Gaussian if there exists a constant $K > 0$ such that*

$$\mathbb{E}\left[\exp\left(\frac{\xi^2}{K^2}\right)\right] \leq 2.$$

The sub-Gaussian norm of ξ is defined to be the smallest K satisfying this inequality.

The class of sub-Gaussian random variables is rich and well-studied. It contains, for example, the Gaussian, uniform, Bernoulli and all bounded random variables, see [45, Example 2.5.8]. In particular, the sub-Gaussian norm of a Gaussian random variable with standard deviation $\delta > 0$ is δ.

We first establish a tail inequality for the operator norm of the matrix Δ, which will be useful for validating the condition (iii) in the master theorem.

Proposition 2. *Suppose that the entries of the noise matrix $(\Theta_{ij})_{k\ell}$, $(i,j) \in E, k, \ell = 1,\dots,d$, are i.i.d. zero-mean sub-Gaussian random variables with sub-Gaussian norm K. Furthermore, suppose that the measurement graph is a random graph that is independent of the noise matrices Θ_{ij}, $(i,j) \in E$, and that satisfies*

$$\hat{r} := (n-1)\max_{i<j} \mathbb{E}\left[w_{ij}\right] \geq 1.$$

Then, there exist numerical constants $c_1, c_2 > 0$ such that

$$\Pr\left(\|\Delta\| \leq sK\sqrt{d\hat{r}}\right) \geq 1 - n(n-1)\exp\left(-d\hat{r}\right) - 2nd\exp\left(-\frac{1}{2}\frac{s^2}{c_1 s + c_2}\right) \quad \forall s > 0.$$

Proof. First, note that for any $i < j$,

$$[\Delta]_{ij} = w_{ij}\left([C]_{ij} - \left[G^* G^{*\top}\right]_{ij}\right) = w_{ij}\left(C_{ij} - G_i^* G_j^{*\top}\right) = w_{ij}\Theta_{ij}.$$

For $i < j$, let $S_{ij} \in \mathbb{R}^{nd\times nd}$ be the symmetric matrix defined by

$$S_{ij} = \begin{pmatrix} & \underbrace{[\Delta]_{ij}}_{(i,j)-\text{th block}} \\ \underbrace{[\Delta]_{ij}^\top}_{(j,i)-\text{th block}} & \end{pmatrix} = w_{ij} \begin{pmatrix} & \Theta_{ij} \\ \Theta_{ij}^\top & \end{pmatrix}.$$

In particular, $\mathbb{E}[S_{ij}] = 0$. Using [45, Theorem 4.4.5] and the fact that $\|S_{ij}\| = \|\Delta_{ij}\|$, there exists a constant $c_1 > 0$ such that

$$\Pr\left(\|S_{ij}\| \le c_1 K(2\sqrt{d} + s'\sqrt{d})\right) \ge 1 - 2\exp\left(-ds'^2\right) \quad \forall s' > 0.$$

Taking $s' = \sqrt{\hat{r}} \ge 1$ and using the union bound, we get

$$\Pr\left(\|S_{ij}\| \le 3c_1 K\sqrt{\hat{r}d} \quad \forall i < j\right) \ge 1 - n(n-1)\exp\left(-\hat{r}d\right). \tag{33}$$

Also, for $i < j$, we have that if $(i, j) \notin E$, $S_{ij}^2 = 0$; and that if $(i, j) \in E$,

$$S_{ij}^2 = \begin{pmatrix} \underbrace{[\Delta]_{ij}[\Delta]_{ij}^\top}_{(i,i)-\text{th block}} & \\ & \underbrace{[\Delta]_{ij}^\top[\Delta]_{ij}}_{(j,j)-\text{th block}} \end{pmatrix} = w_{ij} \begin{pmatrix} \Theta_{ij}\Theta_{ij}^\top & \\ & \Theta_{ij}^\top\Theta_{ij} \end{pmatrix}.$$

By [45, Proposition 2.5.2], the variance of any of the i.i.d. entries of Θ_{ij} is upper bounded by c_2K^2 for some numerical constant $c_2 > 0$. Therefore, we have

$$\mathbb{E}\left[\Theta_{ij}\Theta_{ij}^\top\right], \mathbb{E}\left[\Theta_{ij}^\top\Theta_{ij}\right] \preceq c_2 dK^2 I_d,$$

which implies that

$$\begin{aligned}
\left\|\sum_{i<j} \mathbb{E}\left[S_{ij}^2\right]\right\| &\le c_2 dK^2 \left(\max_{i<j} \mathbb{E}[w_{ij}]\right) \left\|\sum_{i<j} \begin{pmatrix} I_d & \\ & I_d \end{pmatrix}\right\| \\
&= c_2 dK^2 \left(\max_{i<j} \mathbb{E}[w_{ij}]\right) \|(n-1)I_{nd}\| \\
&= c_2 dK^2 \hat{r}
\end{aligned}$$

Since $\Delta = \sum_{i<j} S_{ij}$, it follows from [43, Theorem 6.1.1] that for any $s > 0$,

$$\Pr\left(\|\Delta\| \geq sK\sqrt{d\hat{r}} \;\middle|\; \|S_{ij}\| \leq 3c_1 K \sqrt{\hat{r}d} \quad \forall i < j \right) \leq 2nd \exp\left(-\frac{1}{2} \frac{s^2}{c_2 + c_1 s} \right).$$

By inequality (33) and the law of total probability, for any $s > 0$,

$$\Pr\left(\|\Delta\| \leq sK\sqrt{d\hat{r}} \right) \geq 1 - n(n-1)\exp\left(-d\hat{r}\right) - 2nd \exp\left(-\frac{1}{2} \frac{s^2}{c_2 + c_1 s} \right).$$

This completes the proof. $\square$

The following theorem, which is a substantial generalization of [4, Proposition 3.3], shows that condition (iii) of Theorem 1 is satisfied with high probability if the entries of the noise matrices Θ_{ij} are i.i.d. sub-Gaussian random variables and the measurement graph is Erdös-Rényi.

Theorem 4. *Let $\rho \geq 1$. Suppose that the entries of the noise matrix $(\Theta_{ij})_{k\ell}$, $(i,j) \in E, k, \ell = 1, \ldots, d$, are i.i.d. zero-mean sub-Gaussian random variables with sub-Gaussian norm K. Furthermore, suppose that the synchronization problem has an Erdös-Rényi measurement graph with observation rate $p \geq \frac{1}{n-1}$, which is independent of the noise matrices Θ_{ij}, $(i,j) \in E$. Then, we have*

$$\left\| D^{-1}\Delta \right\| \leq \frac{1}{32\rho} \quad \textit{and} \quad \left\| D^{-1}\Delta G^* \right\|_F \leq \frac{\sqrt{n}}{32\rho}$$

with probability at least

$$1 - \exp\left(-\frac{np^2}{2} + 2p \right) - n(n-1)\exp\left(-dp(n-1)\right) - 2nd \exp\left(-\frac{p(n-1)}{c_1 \rho^2 d^2 K^2 + c_2 \rho d K \sqrt{p(n-1)}} \right).$$

Proof. We first bound $\left\| D^{-1}\Delta \right\|$. Similarly to (30), we can prove that

$$\Pr\left(r_i \geq np(1 - s_1) \right) \geq 1 - \exp(-2s_1^2 np^2 + 4s_1 p) \quad \forall s_1 \in (0,1).$$

Taking $s_1 = \frac{1}{2}$, with probability at least $1 - \exp(-\frac{np^2}{2} + 2p)$, it holds that

$$\left\| D^{-1} \right\| = \max_{i=1,\ldots,n} \frac{1}{r_i} \leq \frac{2}{np}. \tag{34}$$

Next, it follows from the definitions of $\hat{r}$ and Erdös-Rényi measurement graph that $\hat{r} = p(n-1)$. Using Proposition 2 with $s = \sqrt{\hat{r}}/64\rho K d$, there exist some numerical constants $c_1, c_2 > 0$ such that

$$\|\Delta\| \leq \frac{p(n-1)}{64\rho\sqrt{d}} \tag{35}$$

holds with probability at least

$$1 - n(n-1)\exp\left(-dp(n-1)\right) - 2nd\exp\left(-\frac{p(n-1)}{c_1\rho^2 d^2 K^2 + c_2\rho dK\sqrt{p(n-1)}}\right).$$

Combining inequalities (34) and (35), we have

$$\left\|D^{-1}\Delta\right\| \leq \left\|D^{-1}\right\|\|\Delta\| \leq \frac{2}{np}\frac{p(n-1)}{64\rho\sqrt{d}} \leq \frac{1}{32\rho}$$

with probability at least

$$1-\exp\left(-\frac{np^2}{2}+2p\right)-n(n-1)\exp\left(-dp(n-1)\right)-2nd\exp\left(-\frac{p(n-1)}{c_1\rho^2 d^2 K^2 + c_2\rho dK\sqrt{p(n-1)}}\right).$$

To bound $\left\|D^{-1}\Delta G^*\right\|_F$, we first note that $\|G^*\|_F = \sqrt{nd}$ since all of the n blocks G_i^* are $d \times d$ orthogonal matrices. Again using inequalities (34) and (35), we have that

$$\left\|D^{-1}\Delta G^*\right\|_F \leq \left\|D^{-1}\right\|\|\Delta\|\|G^*\|_F \leq \frac{2}{np}\frac{p(n-1)}{64\rho\sqrt{d}}\sqrt{nd} \leq \frac{\sqrt{n}}{32\rho}.$$

This completes the proof. $\square$

In order for the conclusion of Theorem 4 to be non-trivial, the observation rate p should satisfy $p \geq \frac{c}{n^{1/2}}$ for some constant $c > 0$.

8 Spectral Estimator

In order for our non-convex approach to enjoy the theoretical guarantee offered by the master theorem, we need to initialize the GPM by a point G^0 whose estimation error satisfies $\epsilon(G^0) \leq \frac{\sqrt{n}}{2}$. To that end, we propose the initialization

$$G^0 = G_C := \Pi^n(V_C),$$

where $V_C \in \mathbb{R}^{nd\times d}$ is a matrix whose j-th column is the eigenevector associated with the j-th largest eigenvalue of C for $j = 1, \dots, d$. We call G_C the *spectral estimator* of the synchronization problem $\mathcal{G}$-sync. This initialization $G^0 = G_C$ is inspired by and a generalization of the works [7] and [33]. Note that our spectral estimator is slightly different from those in [1] and [38] where each block-row the data matrix C is normalized by the degree of the corresponding node in the measurement graph $([n], E)$. The following proposition provides a general upper bound on the estimation error of the spectral estimator G_C.

Proposition 3. *For any $\eta > 0$, we have*

$$\epsilon(G_C) \leq \frac{4\sqrt{2}\sqrt{d}}{\eta\sqrt{n}} \left\| C - \eta \cdot G^* {G^*}^\top \right\|.$$

The proof of Proposition 3 relies on the following version of Davis-Kahan Theorem [48].

Theorem 5. *Let $M, M^* \in \mathbb{R}^{N\times N}$ be symmetric matrices with eigenvalues $\lambda_1 \geq \cdots \geq \lambda_N$ and $\lambda_1^* \geq \cdots \geq \lambda_N^*$, respectively. For any integers k, ℓ such that $1 \leq k \leq \ell \leq N$, let $V, V^* \in \mathbb{R}^{N\times(\ell-k+1)}$ be the matrices defined by*

$$V = \begin{pmatrix} | & & | \\ v_k & \cdots & v_\ell \\ | & & | \end{pmatrix} \quad \text{and} \quad V^* = \begin{pmatrix} | & & | \\ v_k^* & \cdots & v_\ell^* \\ | & & | \end{pmatrix},$$

where v_i and v_i^* are respectively the eigenvectors of M and M^* corresponding to the eigenvalues λ_i and λ_i^*, $i = 1, \ldots, N$. Suppose that $\min\{\lambda_{k-1}^* - \lambda_k^*, \lambda_\ell^* - \lambda_{\ell+1}^*\} > 0$, where $\lambda_0 = +\infty$, $\lambda_{N+1} = -\infty$. Then, there exists $Q^* \in \mathcal{O}(\ell - k + 1)$ such that

$$\|V - V^* Q^*\|_F \leq \frac{2\sqrt{2}\min\{\sqrt{\ell-k+1}\,\|M - M^*\|, \|M - M^*\|_F\}}{\min\{\lambda_{k-1}^* - \lambda_k^*, \lambda_\ell^* - \lambda_{\ell+1}^*\}}$$

We can now prove Proposition 3.

Proof of Proposition 3. Note that the columns of $\frac{1}{\sqrt{n}}G^*$ are the eigenvectors of $\eta \cdot G^* {G^*}^\top$, all with eigenvalues ηn. Applying Theorem 5 with $M = C$, $M^* = \eta \cdot G^* {G^*}^\top$, $k = 1$ and $\ell = d$, there exists a matrix $Q^* \in \mathcal{O}(d)$ such that

$$\begin{aligned} \left\| V_C - \frac{1}{\sqrt{n}} G^* Q^* \right\|_F &\leq \frac{2\sqrt{2}\min\left\{\sqrt{d}\left\|C - \eta \cdot G^* {G^*}^\top\right\|, \left\|C - \eta \cdot G^* {G^*}^\top\right\|_F\right\}}{\min\{\lambda_{k-1}^* - \lambda_k^*, \lambda_\ell^* - \lambda_{\ell+1}^*\}} \\ &\leq \frac{2\sqrt{2}\sqrt{d}\left\|C - \eta \cdot G^* {G^*}^\top\right\|}{\eta n}. \end{aligned} \tag{36}$$

Similarly to (8), we can show that

$$\|\Pi([V_C]_i) - G_i^* Q^*\|_F \leq 2\left\|\sqrt{n}[V_C]_i - G_i^* Q^*\right\|_F \quad \forall i = 1, \ldots, n. \tag{37}$$

Using inequalities (36) and (37), we have

$$\begin{aligned} \epsilon(G_C) &= \min_{Q\in\mathcal{O}(d)} \|G_C - G^* Q\|_F \leq \|\Pi^n(V_C) - G^* Q^*\|_F \\ &\leq 2\sqrt{n}\left\|V_C - \frac{1}{\sqrt{n}} G^* Q^*\right\|_F \leq \frac{4\sqrt{2}\sqrt{d}\left\|C - \eta \cdot G^* {G^*}^\top\right\|}{\eta\sqrt{n}}. \end{aligned}$$

This completes the proof. $\square$

The following theorem verifies condition (iv) in the master theorem for the spectral initialization, under the setting of sub-Gaussian noise and Erdös-Rényi measurement graph.

Theorem 6. *Under the conditions of Theorem 4, we have*

$$\epsilon(G_C) \leq \frac{\sqrt{n}}{2\rho}$$

with probability at least

$$1-2nd\exp\left(\frac{-pn}{c_1\rho^2 d}\right)-n(n-1)\exp\left(-dp(n-1)\right)-2nd\exp\left(-\frac{p(n-1)}{c_2\rho^2 d^2 K^2 + c_3\rho d K\sqrt{p(n-1)}}\right).$$

Proof. Let $C^* \in \mathbb{R}^{nd\times nd}$ be the block matrix defined by $[C^*]_{ij} = w_{ij} G_i^* G_j^{*\top}$, $i, j = 1, \ldots, n$, and $\Delta^* = C^* - p \cdot G^* G^{*\top}$. By definition, $C - C^* = \Delta$ and

$$\Delta^* = \sum_{i<j} (w_{ij} - p) R_{ij},$$

where, for $i < j$, $R_{ij} \in \mathbb{R}^{nd\times nd}$ is defined as

$$R_{ij} = \begin{pmatrix} & & \underbrace{G_i^* G_j^{*\top}}_{(i,j)-\text{th block}} & \\ & & & \\ & \underbrace{G_j^* G_i^{*\top}}_{(j,i)-\text{th block}} & & \\ & & & \end{pmatrix}.$$

We first bound $\|\Delta^*\|$. To this end, we observe that $\|R_{ij}\| = \left\|G_i^* G_j^{*\top}\right\| = 1$ which implies that $\|(w_{ij} - p)R_{ij}\| \leq \max\{p, 1-p\}$. Furthermore, since

$$(w_{ij} - p)^2 R_{ij}^2 = (w_{ij} - p)^2 \begin{pmatrix} I_d & \\ & I_d \end{pmatrix},$$

we have that

$$\left\| \sum_{i<j} \mathbb{E}\left[(w_{ij}-p)^2 R_{ij}^2\right] \right\| = \left\| \sum_{i<j} \mathbb{E}\left[(w_{ij}-p)^2 \begin{pmatrix} I_d & \\ & I_d \end{pmatrix} \right] \right\|$$
$$= \left\| \mathbb{E}\left[(w_{ij}-p)^2\right](n-1) I_{nd} \right\|$$
$$= p(1-p)(n-1).$$

It follows from [43, Theorem 6.1.1] that for any $s > 0$,

$$\Pr\left(\|\Delta^*\| \geq s\right) \leq 2nd \exp\left(-\frac{1}{2}\frac{s^2}{p(1-p)(n-1)+\max\{p,1-p\}s/3}\right).$$

Therefore, there exists a numerical constant $c_1 > 0$ such that

$$\Pr\left(\|\Delta^*\| \geq \frac{pn}{16\sqrt{2}\rho\sqrt{d}}\right) \leq 2nd \exp\left(\frac{-pn}{c_1\rho^2 d}\right). \tag{38}$$

Also, using Proposition 2 with $s = \sqrt{\hat{r}}/16\sqrt{2}\rho K d$, there exist some numerical constants $c_2, c_3 > 0$ such that

$$\begin{aligned} &\Pr\left(\|\Delta\| \geq \frac{p(n-1)}{16\sqrt{2}\rho\sqrt{d}}\right) \\ &\leq n(n-1)\exp\left(-dp(n-1)\right) + 2nd\exp\left(-\frac{p(n-1)}{c_2\rho^2 d^2 K^2 + c_3\rho d K\sqrt{p(n-1)}}\right). \end{aligned} \tag{39}$$

Hence, by Proposition 3 and inequalities (38) and (39), we have

$$\begin{aligned} \epsilon(G_C) &\leq \frac{4\sqrt{2}\sqrt{d}}{p\sqrt{n}} \left\| C - p\cdot G^* G^{*\top} \right\| \\ &\leq \frac{4\sqrt{2}\sqrt{d}}{p\sqrt{n}} \left(\|\Delta\| + \|\Delta^*\|\right) \\ &\leq \frac{4\sqrt{2}\sqrt{d}}{p\sqrt{n}} \left(\frac{p(n-1)}{16\sqrt{2}\rho\sqrt{d}} + \frac{pn}{16\sqrt{2}\rho\sqrt{d}}\right) \\ &\leq \frac{\sqrt{n}}{2\rho} \end{aligned}$$

with probability at least

$$1 - 2nd\exp\left(\frac{-pn}{c_1\rho^2 d}\right) - n(n-1)\exp\left(-dp(n-1)\right) - 2nd\exp\left(-\frac{p(n-1)}{c_2\rho^2 d^2 K^2 + c_3\rho d K\sqrt{p(n-1)}}\right).$$

This completes the proof. □

In order for the conclusion of Theorem 6 to be non-trivial, the observation rate p should satisfy $p \geq \frac{c}{n}$ for some constant $c > 0$.

Very recently, tighter bounds for the estimation error of the spectral estimator G_C are obtained in [27] via the *leave-one-out* technique. Their bounds are only for $\mathcal{P}(d)$-sync under the outlier noise model and $\mathcal{O}(d)$-sync under the additive Gaussian noise model, both with full observations, *i.e.*, $p = 1$. Our weaker bound is applicable to a general closed subgroup $\mathcal{G}$ of the orthogonal group under general observation rate p and additive sub-Gaussian noise. Nevertheless, the goal here is to devise, in a unified manner, an initialization for GPM that satisfies the estimation error requirement in the master theorem.

9 Numerical Experiments

Numerical experiments are performed in this section to demonstrate the superiority of algorithm in terms of computational speed, scalability and estimation performance. All the codes are implemented using MATLAB and tested on a 2019 Lenovo ThinkPad X1 Carbon with the Intel Core i7-10510U (1.80GHz×4).

9.1 Special Orthogonal Synchronization

We first present our experiments on $\mathcal{SO}(d)$-sync.

9.1.1 Experiment Setting

We focus on the case of $d = 3$, which is most relevant to applications. The experiment setting, which is the same as in [46], is as follows. For the measurement graph $([n], E)$, we use the Erdös-Rényi graph with observation rate $p \in (0, 1]$. We consider a multiplicative noise model with two layers of multiplicative noise. More precisely, we generate our observations C_{ij} as

$$C_{ij} = G_i^* G_j^{*\top} \Theta_{ij}^{\text{out}} \Theta_{ij}^{\text{Lang}} \quad \forall (i,j) \in E,$$

where Θ_{ij}^{out} is the so-called outlier noise defined by

$$\Theta_{ij}^{\text{out}} = \begin{cases} I_d & \text{with probability } q, \\ Q_{ij} \sim \text{Uniform}(\mathcal{SO}(3)) & \text{with probability } 1 - q, \end{cases}$$

where $q \in (0, 1]$, Uniform$(\mathcal{SO}(3))$ is the uniform distribution on $\mathcal{SO}(3)$, and $\Theta_{ij}^{\text{Lang}} \in \mathcal{SO}(3)$ is generated by the Langevin distribution (also called the von Mises-Fisher distribution) [14, 46] on $\mathcal{SO}(3)$ with mean I_d and concentration parameter $\gamma \geq 0$, *i.e.*, the density function of each $\Theta_{ij}^{\text{Lang}}$ is given by

$$c(\gamma) \exp\left(\gamma \operatorname{Tr}(\Theta_{ij}^{\text{Lang}})\right),$$

for some normalization constant $c(\gamma) > 0$. The parameter $\gamma \geq 0$ controls the concentration of the random matrix $\Theta_{ij}^{\mathrm{Lang}}$ around the mean I_d — the larger the parameter γ is, the more concentrated around the mean I_d the random matrix $\Theta_{ij}^{\mathrm{Lang}}$ is. In particular, it is the uniform distribution Uniform($\mathcal{SO}(3)$) when $\gamma = 0$. As $\gamma \to +\infty$, the distribution behaves like a Gaussian distribution with mean I_d and variance $\frac{1}{\gamma}$.

9.1.2 Experiment Results

We compare our approach with the least unsquared deviation approach in [46] and the low-rank-sparse decomposition approach in [2]. We also include the spectral estimator in the comparison as baseline. The codes for the least unsquared deviation approach are provided by the authors; and those for the low-rank-sparse decomposition approach are available at the authors' website. In our experiments, we use the default choice for all the parameters of their codes. Since both of the two competing methods are known to perform well against outlier noise, we mainly study the recovery performance as measured by the estimation error $\epsilon(\,\cdot\,)$ (see (2)) and the computational time by varying the proportion of outliers $1 - q$. Figures 2 and 3 show the experiment results in the low noise ($\gamma = 5$) and high noise ($\gamma = 1$) regimes, respectively. For the computational time, since our non-convex approach is initialized by the spectral estimator, the time for our approach shown in the figures includes the time for computing the spectral estimator. All the points in the figures are obtained as the average over 30 independent random instances.

From Figure 2, we can see that our non-convex approach performs generally on par with the low-rank-sparse decomposition approach in terms of both estimation error and computation time, except for the case $p = 0.2$ where our method is faster. Despite that the spectral estimator is shown to be already rate-optimal under some settings [7, 27] and that our non-convex approach is initialized by the spectral estimator, the estimation error of the non-convex approach is substantially better than that of the spectral estimator. Quite surprisingly, the least unsquared deviation approach performs worse than the spectral estimator in terms of estimation error. The optimization problem associated with the least unsquared deviation approach is a nonlinear convex semidefinite programming obtained via relaxation technique and solved by the alternating direction augmented Lagrangian method [47]. We suspect that the unsatisfactory performance of the least unsquared deviation approach might be due to the fact that the alternating direction augmented Lagrangian method can only achieve low to medium accuracy and/or is sensitive to the penalty parameter in the augmented Lagrangian term.

The results in the high noise regime are shown in Figure 3. Similar behavior as in the low noise regime are observed for the spectral approach and the least unsquared deviation approach. Compared with the low-rank-sparse decomposition approach, our non-convex approach is fairly faster in this regime and at the same time has slightly better estimation error. This suggests that the proposed non-convex approach is very robust against multiplicative noise, although our theory does not cover such a noise setting.

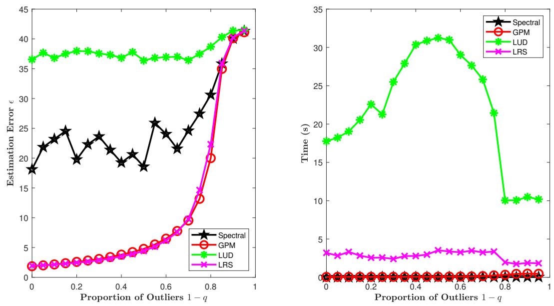

(a) $n = 300, d = 3, p = 0.2, \gamma = 5$

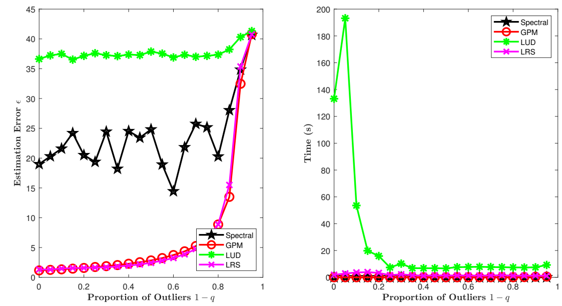

(b) $n = 300, d = 3, p = 0.5, \gamma = 5$

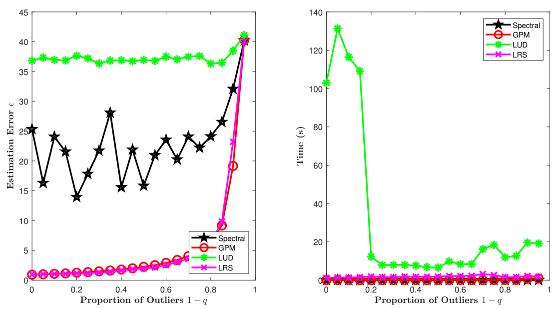

(c) $n = 300, d = 3, p = 0.8, \gamma = 5$

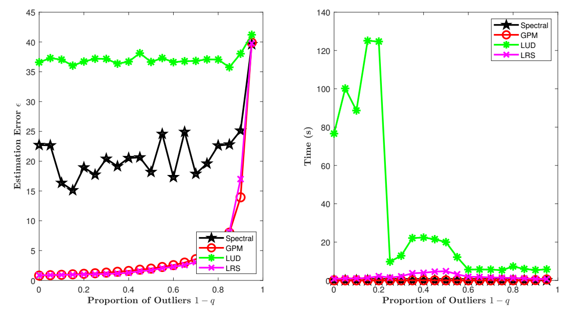

(d) $n = 300, d = 3, p = 1, \gamma = 5$

Figure 2: Estimation error and computational time of our non-convex approach (labeled as GPM), the spectral estimator (labeled as Spectral), the least unsquared deviation approach (labeled as LUD) and the low-rank-sparse decomposition approach (labeled as LRS) under low Langevin noise ($\gamma = 5$) and observation rate $p = 0.2, 0.5, 0.8, 1$.

9.2 Permutation Synchronization

Next, we investigate the numerical performance of our approach for solving the permutation synchronization problem, *i.e.*, $\mathcal{P}(d)$-sync.

9.2.1 Experiment Setting

We focus on the setting where the measurement graph is the Erdös-Rényi graph with observation rate $p \in (0, 1)$ and the measurements are given by

$$C_{ij} = \Pi_{\mathcal{P}(d)}(G_i^* G_j^{*\top} + \delta\, W_{ij}) \quad \forall (i, j) \in E,$$

where each $W_{ij} \in \mathbb{R}^{d \times d}$ is a random matrix with i.i.d. standard Gaussian entries and $\delta > 0$ is parameter controlling the magnitude of the noise. Due to the discrete nature of the signals (permutation matrices), instead of the estimation error $\epsilon(\,\cdot\,)$, we quantify the

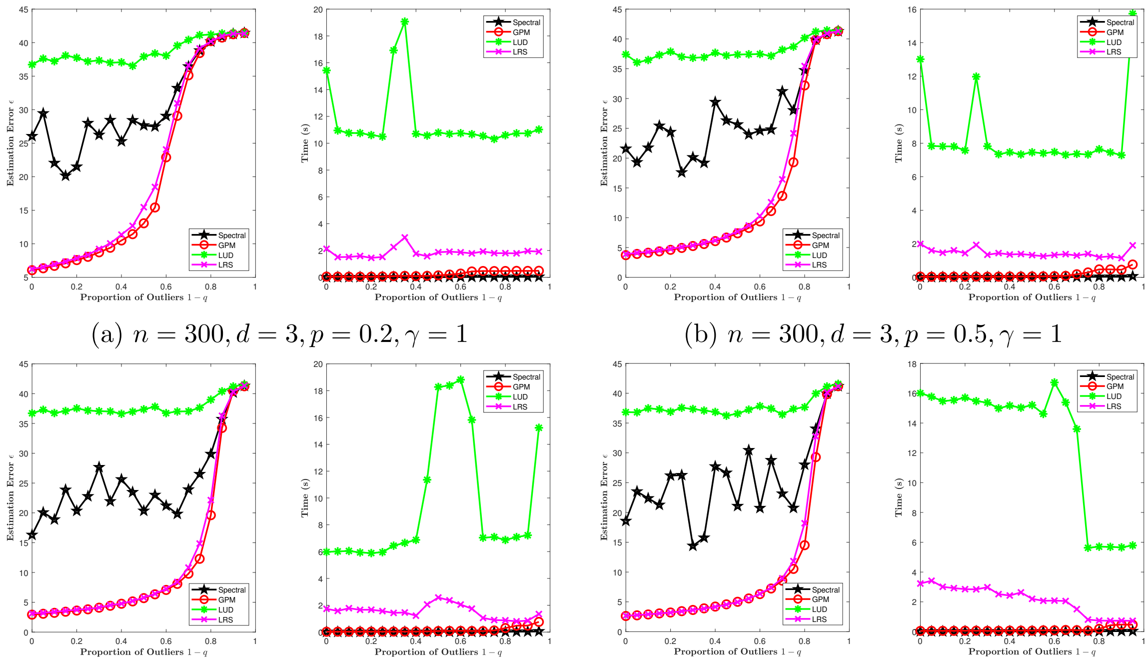

(a) $n = 300, d = 3, p = 0.2, \gamma = 1$

(b) $n = 300, d = 3, p = 0.5, \gamma = 1$

(c) $n = 300, d = 3, p = 0.8, \gamma = 1$

(d) $n = 300, d = 3, p = 1, \gamma = 1$

Figure 3: Estimation error and computational time of our non-convex approach (labeled as GPM), the spectral estimator (labeled as Spectral), the least unsquared deviation approach (labeled as LUD) and the low-rank-sparse decomposition approach (labeled as LRS) under high Langevin noise ($\gamma = 1$) and observation rate $p = 0.2, 0.5, 0.8, 1$.

estimation performance by the *recovery rate*, which is defined as

$$\text{Recovery Rate} = \frac{\text{number of correctly recovered group elements}}{n}. \tag{40}$$

9.2.2 Experiment Results

We compare our approach with the "relaxed algorithm" in [33], which coincides with the spectral estimator G_C, and the iterative approach based on QR factorization developed in [38] by varying the parameters n and d. All the points in the figures are obtained as the average over 30 independent random instances.

As we can see from Figures 4 and 5, the recovery performance of our non-convex approach is significantly better than that of the spectral estimator and the QR factorization-based approach. Furthermore, compared with the QR factorization-based approach, our non-convex approach required a shorter computational time in Figure 4 (where we varied n) and roughly the same computational time in Figure 5 (where we varied d). Of course

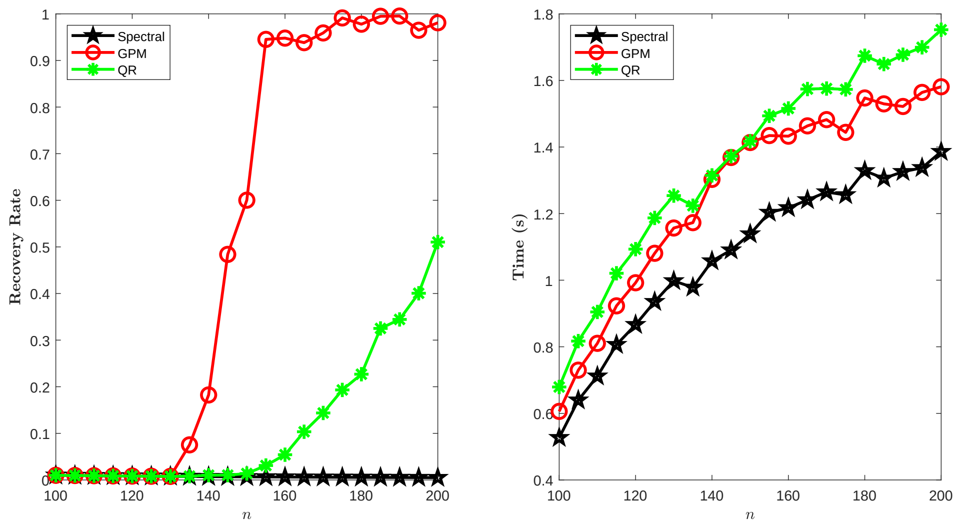

Figure 4: Recovery rate and computational time (in second) of the spectral estimator (labeled as Spectral), the proposed non-convex approach (labeled as GPM) and the QR factorization-based approach (labeled as QR) for $d = 20$, $p = 0.5$, $q = 0.8$, $\delta = 1$ and $n = 100, 105, \ldots, 200$.

the computational time of the spectral estimator is the shortest among the three tested methods, since both the non-convex approach and the QR factorization-based approach are initialized by the spectral estimator.

9.3 Cyclic Synchronization (Joint Alignment Problem)

Finally, we present our experiments on cyclic synchronization, *i.e.*, synchronization over the cyclic group $\mathcal{Z}_m$. This is also equivalent to the joint alignment problem [13].

9.3.1 Experiment Setting

We adopt the same experiment setting as in [13]. Specifically, we consider the Erdös-Rényi measurement graph with observation rate $p \in (0, 1)$. For the error model, each observation C_{ij} is corrupted by the multiplicative outlier noise with corruption probability $1 - q \in [0, 1)$:

$$C_{ij} = G_i^* G_j^{*\top} \Theta_{ij}^{\text{out}} \quad \forall (i, j) \in E,$$

where

$$\Theta_{ij}^{\text{out}} = \begin{cases} I_2 & \text{with probability } q, \\ Q_k & \text{with probability } 1 - q, \end{cases}$$

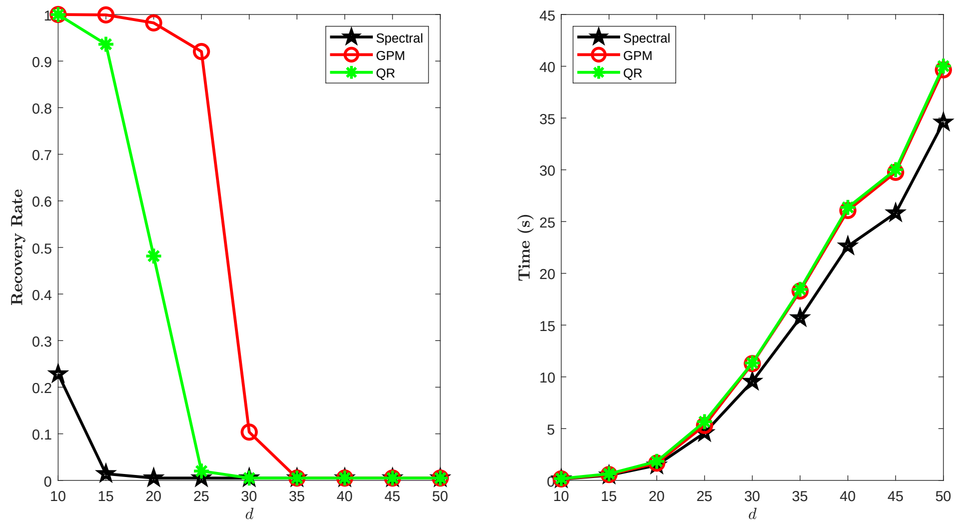

Figure 5: Recovery rate and computational time (in second) of the spectral estimator (labeled as Spectral), the proposed non-convex approach (labeled as GPM) and the QR factorization-based approach (labeled as QR) for $n = 200$, $p = 0.5$, $q = 0.8$, $\delta = 1$ and $d = 10, 15, \ldots, 50$.

Q_k is defined in (19) and $k \sim \text{Uniform}([m])$. To quantify the estimation performance, we use again the recovery rate[4] defined in (40).

9.3.2 Experiment Results

The proposed non-convex approach is compared against another non-convex approach developed in [13], named the projected power method. The spectral estimator for $\mathcal{Z}_m$-sync is once again included in the experiments as a baseline. We focus on how the recovery rate and computation time of these approaches depend on the cyclic group order m. The experiment results are plotted in Figure 6. All the points in the figure are obtained as the average over 30 independent random instances.

In terms of computational time, the proposed non-convex approach significantly outperforms the projected power method. For the recovery performance, our approach is worse than the projected power method, especially when the group order m is large (see Figures 6(a) and 6(c).) Therefore, for cyclic synchronization problems, the projected power method is the way to go if we are focusing on the recovery performance. However, if speed

[4] In [13], the *misclassification rate* is used to quantify the estimation performance, which is equal to 1-Recovery Rate.

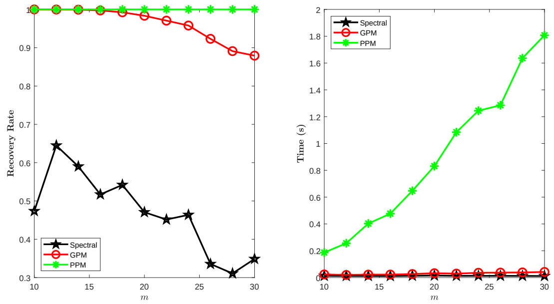

(a) $n = 500, p = 0.5, q = 0.5$

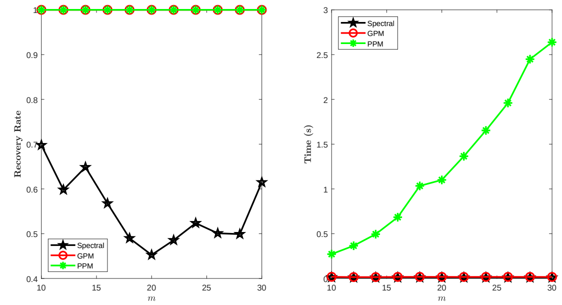

(b) $n = 500, p = 0.5, q = 0.8$

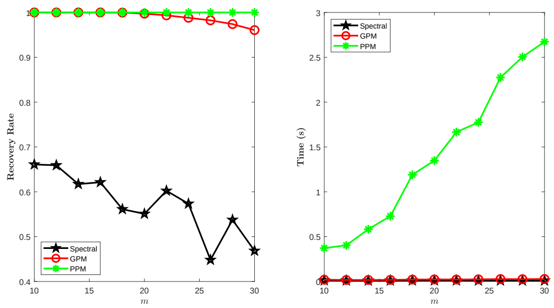

(c) $n = 500, p = 0.8, q = 0.5$

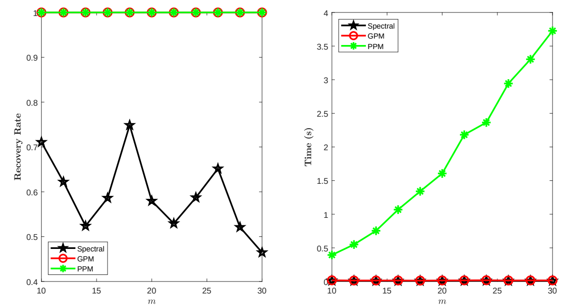

(d) $n = 500, p = 0.8, q = 0.8$

Figure 6: Recovery rate and computational time of our non-convex approach (labeled as GPM), the spectral estimator (labeled as Spectral) and the projected power method (labeled as PPM) for observation rates $p = 0.5, 0.8$ and non-corruption rates $q = 0.5, 0.8$.

and scalability are of great concern, our experiment results suggest that the proposed non-convex approach would be a better alternative.

10 Conclusions

In this paper, we studied the class of synchronization problems over subgroups of the orthogonal group. As our first main contribution, we proposed a unified approach to tackle this class of synchronization problems. The proposed approach consists of a suitable initialization and an iterative refinement stage based on the generalized power method. Our second contribution lies in the derivation of the master theorem which shows that the estimation error of the iterates produced by our approach decreases geometrically under certain conditions. Finally, we verified the conditions of the master theorem for specific examples of the subgroups, the measurement graph, the noise model and the initialization by a novel spectral estimator that we proposed. Our experiment results showed that the proposed approach outperforms existing approaches in terms of computational speed, scalability and estimation error.

Besides Conjecture 1, there are two other research questions regarding solving group synchronization problems by non-convex approaches that are worth investigating. First, although our theory in Section 7 covers only additive noise models but not multiplicative ones, experiments showed that the proposed approach works efficiently for the outlier noise model which is multiplicative. Thus, an obvious research problem would be to extend the analysis to cover multiplicative noise models. Second, an important example of group synchronization problems is the $SE(d)$-sync [37], where $SE(d)$ is the group of Euclidean motions, and arises from areas such as robotics and computer vision. The group $SE(d)$ is not a subgroup of the orthogonal group. It would be interesting to see whether a similar non-convex approach can be developed for solving $SE(d)$-sync.

Acknowledgment

We thank Mihai Cucuringu, Yin-Tat Lee and Michael Kwok-Po Ng for helpful discussions and Amit Singer for kindly sharing with us their codes for the experiments.

References

[1] M. Arie-Nachimson, S. Z. Kovalsky, I. Kemelmacher-Shlizerman, A. Singer, and R. Basri. Global motion estimation from point matches. In *2012 Second International Conference on 3D Imaging, Modeling, Processing, Visualization & Transmission*, pages 81–88. IEEE, 2012.

[2] F. Arrigoni, B. Rossi, P. Fragneto, and A. Fusiello. Robust synchronization in SO(3) and SE(3) via low-rank and sparse matrix decomposition. *Computer Vision and Image Understanding*, 174:95–113, 2018.

[3] A. S. Bandeira. Random laplacian matrices and convex relaxations. *Foundations of Computational Mathematics*, 18(2):345–379, 2018.

[4] A. S. Bandeira, N. Boumal, and A. Singer. Tightness of the maximum likelihood semidefinite relaxation for angular synchronization. *Mathematical Programming*, 163(1-2):145–167, 2017.

[5] A. S. Bandeira, N. Boumal, and V. Voroninski. On the low-rank approach for semidefinite programs arising in synchronization and community detection. In *Conference on Learning Theory*, pages 361–382, 2016.

[6] A. S. Bandeira, A. Singer, and D. A. Spielman. A Cheeger inequality for the graph connection Laplacian. *SIAM Journal on Matrix Analysis and Applications*, 34(4):1611–1630, 2013.

[7] N. Boumal. Nonconvex phase synchronization. *SIAM Journal on Optimization*, 26(4):2355–2377, 2016.

[8] N. Boumal, V. Voroninski, and A. Bandeira. The non-convex Burer-Monteiro approach works on smooth semidefinite programs. In *Advances in Neural Information Processing Systems*, pages 2757–2765, 2016.

[9] N. Boumal, V. Voroninski, and A. S. Bandeira. Deterministic guarantees for Burer-Monteiro factorizations of smooth semidefinite programs. *Communications on Pure and Applied Mathematics*, 73(3):581–608, 2020.

[10] S. Burer and R. D. Monteiro. A nonlinear programming algorithm for solving semidefinite programs via low-rank factorization. *Mathematical Programming*, 95(2):329–357, 2003.

[11] S. Burer and R. D. Monteiro. Local minima and convergence in low-rank semidefinite programming. *Mathematical Programming*, 103(3):427–444, 2005.

[12] R. Burkard, M. Dell'Amico, and S. Martello. *Assignment Problems (Revised Reprint)*, volume 106. SIAM, 2012.

[13] Y. Chen and E. J. Candès. The projected power method: An efficient algorithm for joint alignment from pairwise differences. *Communications on Pure and Applied Mathematics*, 71(8):1648–1714, 2018.

[14] A. Chiuso, G. Picci, and S. Soatto. Wide-sense estimation on the special orthogonal group. *Communications in Information & Systems*, 8(3):185–200, 2008.

[15] M. Cucuringu. Synchronization over Z_2 and community detection in signed multiplex networks with constraints. *Journal of Complex Networks*, 3(3):469–506, 2015.

[16] M. Cucuringu. Sync-Rank: Robust ranking, constrained ranking and rank aggregation via eigenvector and SDP synchronization. *IEEE Transactions on Network Science and Engineering*, 3(1):58–79, 2016.

[17] M. Cucuringu, A. Singer, and D. Cowburn. Eigenvector synchronization, graph rigidity and the molecule problem. *Information and Inference: A Journal of the IMA*, 1(1):21–67, 2012.

[18] M. Fanuel and H. Tyagi. Denoising modulo samples: k-NN regression and tightness of SDP relaxation. *arXiv preprint arXiv:2009.04850*, 2020.

[19] A. Giridhar and P. R. Kumar. Distributed clock synchronization over wireless networks: Algorithms and analysis. In *Decision and Control, 2006 45th IEEE Conference on*, pages 4915–4920. IEEE, 2006.

[20] G. H. Golub and C. F. Van Loan. *Matrix Computations*. Johns Hopkins University Press, 4th edition, 2013.

[21] J. C. Gower and G. B. Dijksterhuis. *Procrustes Problems*, volume 30. Oxford University Press on Demand, 2004.

[22] Q.-X. Huang and L. Guibas. Consistent shape maps via semidefinite programming. In *Computer Graphics Forum*, volume 32, pages 177–186. Wiley Online Library, 2013.

[23] A. Javanmard, A. Montanari, and F. Ricci-Tersenghi. Phase transitions in semidefinite relaxations. *Proceedings of the National Academy of Sciences*, 113(16):E2218–E2223, 2016.

[24] M. Journée, Y. Nesterov, P. Richtárik, and R. Sepulchre. Generalized power method for sparse principal component analysis. *Journal of Machine Learning Research*, 11(Feb):517–553, 2010.

[25] W. Kabsch. A discussion of the solution for the best rotation to relate two sets of vectors. *Acta Crystallographica Section A: Crystal Physics, Diffraction, Theoretical and General Crystallography*, 34(5):827–828, 1978.

[26] G. Lerman and Y. Shi. Robust group synchronization via cycle-edge message passing. *arXiv preprint arXiv:1912.11347*, 2019.

[27] S. Ling. Near-optimal performance bounds for orthogonal and permutation group synchronization via spectral methods. *arXiv preprint arXiv:2008.05341*, 2020.

[28] S. Ling. Solving orthogonal group synchronization via convex and low-rank optimization: Tightness and landscape analysis. *arXiv preprint arXiv:2006.00902*, 2020.

[29] H. Liu, M.-C. Yue, and A. Man-Cho So. On the estimation performance and convergence rate of the generalized power method for phase synchronization. *SIAM Journal on Optimization*, 27(4):2426–2446, 2017.

[30] H. Liu, M.-C. Yue, A. M.-C. So, and W.-K. Ma. A discrete first-order method for large-scale MIMO detection with provable guarantees. In *2017 IEEE 18th International Workshop on Signal Processing Advances in Wireless Communications (SPAWC)*, pages 1–5. IEEE, 2017.

[31] Z.-Q. Luo, W.-K. Ma, A. M.-C. So, Y. Ye, and S. Zhang. Semidefinite relaxation of quadratic optimization problems. *IEEE Signal Processing Magazine*, 27(3):20–34, 2010.

[32] R. Luss and M. Teboulle. Conditional gradient algorithms for rank-one matrix approximations with a sparsity constraint. *SIAM Review*, 55(1):65–98, 2013.

[33] D. Pachauri, R. Kondor, and V. Singh. Solving the multi-way matching problem by permutation synchronization. In *Advances in Neural Information Processing Systems*, pages 1860–1868, 2013.

[34] A. Perry, A. S. Wein, A. S. Bandeira, and A. Moitra. Optimality and sub-optimality of PCA I: Spiked random matrix models. *The Annals of Statistics*, 46(5):2416–2451, 2018.

[35] E. Romanov and M. Gavish. The noise-sensitivity phase transition in spectral group synchronization over compact groups. *Applied and Computational Harmonic Analysis*, 2019.

[36] J. S. Rose. *A Course on Group Theory*. Courier Corporation, 1994.

[37] D. M. Rosen, L. Carlone, A. S. Bandeira, and J. J. Leonard. SE-Sync: A certifiably correct algorithm for synchronization over the special Euclidean group. *The International Journal of Robotics Research*, 38(2-3):95–125, 2019.

[38] Y. Shen, Q. Huang, N. Srebro, and S. Sanghavi. Normalized spectral map synchronization. In *Advances in Neural Information Processing Systems*, pages 4925–4933, 2016.

[39] Y. Shkolnisky and A. Singer. Viewing direction estimation in Cryo-EM using synchronization. *SIAM Journal on Imaging Sciences*, 5(3):1088–1110, 2012.

[40] H. Si, H. Vikalo, and S. Vishwanath. Haplotype assembly: An information theoretic view. In *Information Theory Workshop (ITW), 2014 IEEE*, pages 182–186. IEEE, 2014.

[41] A. Singer. Angular synchronization by eigenvectors and semidefinite programming. *Applied and Computational Harmonic Analysis*, 30(1):20–36, 2011.

[42] L. Trevisan. Max cut and the smallest eigenvalue. *SIAM Journal on Computing*, 41(6):1769–1786, 2012.

[43] J. A. Tropp. An introduction to matrix concentration inequalities. *Foundations and Trends® in Machine Learning*, 8(1-2):1–230, 2015.

[44] H. Tyagi. Error analysis for denoising smooth modulo signals on a graph. *arXiv preprint arXiv:2009.04859*, 2020.

[45] R. Vershynin. *High-dimensional Probability: An Introduction with Applications in Data Science*, volume 47. Cambridge University Press, 2018.

[46] L. Wang and A. Singer. Exact and stable recovery of rotations for robust synchronization. *Information and Inference: A Journal of the IMA*, 2(2):145–193, 2013.

[47] Z. Wen, D. Goldfarb, and W. Yin. Alternating direction augmented Lagrangian methods for semidefinite programming. *Mathematical Programming Computation*, 2(3-4):203–230, 2010.

[48] Y. Yu, T. Wang, and R. J. Samworth. A useful variant of the Davis–Kahan theorem for statisticians. *Biometrika*, 102(2):315–323, 2015.

[49] Y. Zhong and N. Boumal. Near-optimal bounds for phase synchronization. *SIAM Journal on Optimization*, 28(2):989–1016, 2018.